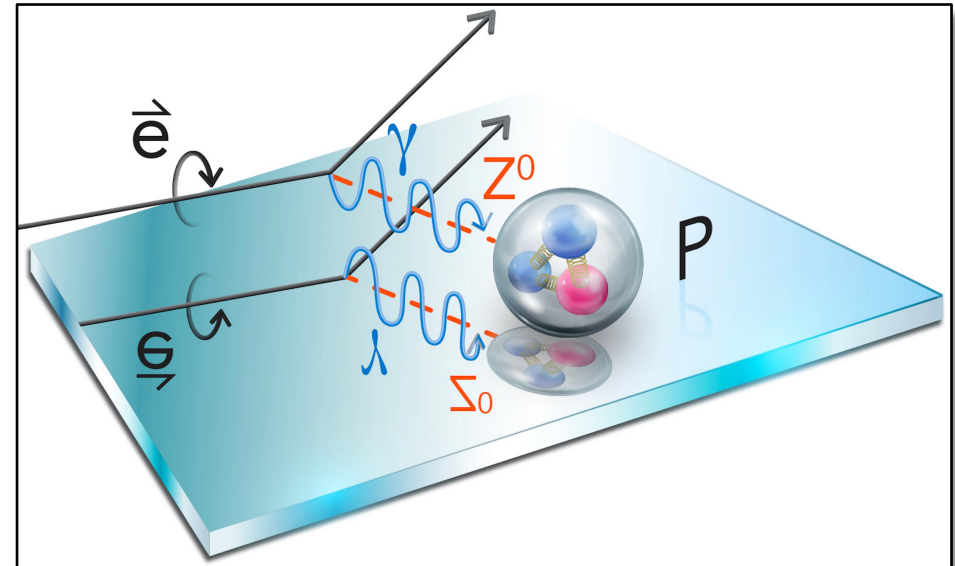
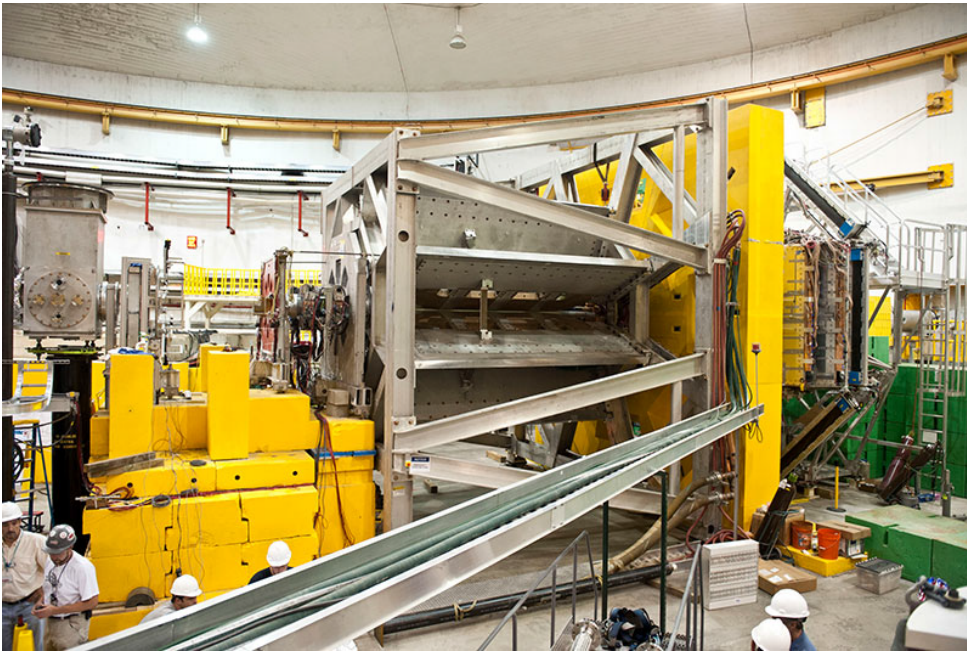


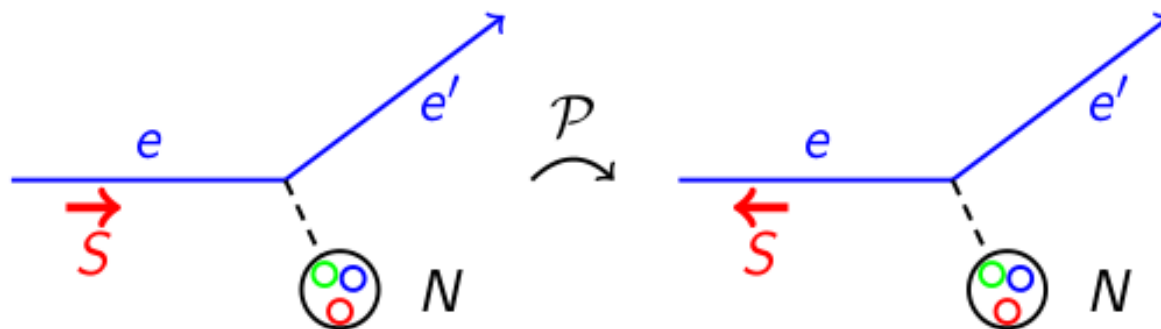
Final Results from the Q_{weak} Experiment: A Search for New Physics via a Measurement of the Proton's Weak Charge

Mark Pitt, Virginia Tech
for the Q_{weak} Collaboration

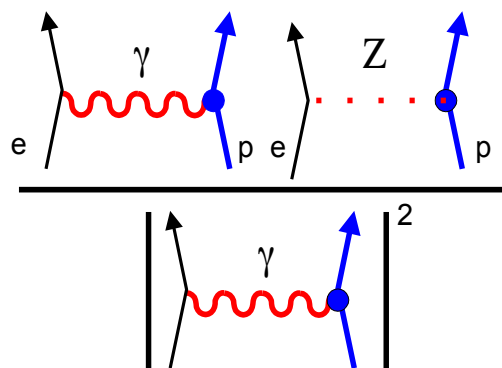
Jefferson Lab Physics Seminar
September 8, 2017



Parity-Violating Electron Scattering – The Basics



$$A = \frac{\sigma_R - \sigma_L}{\sigma_R + \sigma_L} \propto$$



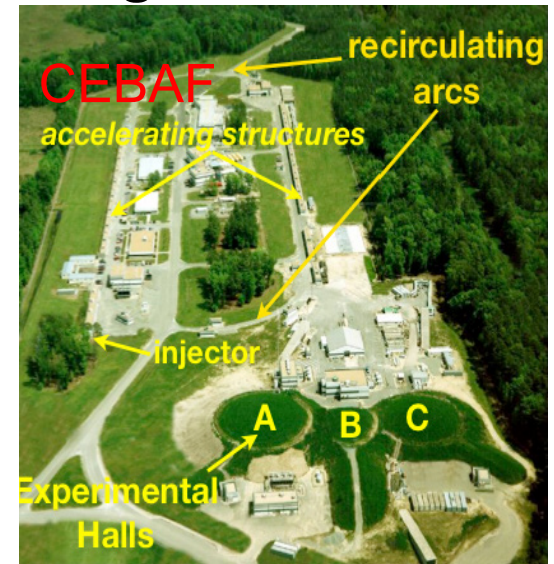
- Longitudinally polarized electrons on unpolarized targets –
e, **p**, d, ⁴He, ⁹Be, ¹²C, ²⁰⁸Pb
- Measure small parity-violating cross section asymmetry
(~ 20 ppb – 100 ppm) **~ -230 ppb (part per billion) for Q_{weak}**
- **Elastic** and deep inelastic kinematics
- **Neutral weak current – Standard Model test** and select hadronic physics topics

Q_{weak} Experiment at Jefferson Lab

Q_{weak} **Collaboration:** 101 collaborators, 26 graduate students, 11 postdocs, 27 institutions

Q_{weak} Experiment: parity-violating e-p elastic scattering to measure proton's weak charge

- Initial organizational meeting 2000
- Proposal 2001
- Design/construction 2003 – 2010
- Data-taking 2010 – 2012 (~ 1 year total beam time)
- Last experiment in Hall C in “6 GeV era”
- First results on proton's weak charge (based on 4% of the dataset) published in **Phys. Rev. Lett. 111, 141803 (2013)**
- Apparatus described in **NIM A781, 105 (2015)**
- Final analysis and unblinding completed; final results first released at 21st Particles & Nuclei International Conference (PANIC) in Beijing, China by Roger Carlini on September 3, 2017



Outline

- Motivation and formalism
- Experiment: technical challenges and achievements
- Analysis: Key systematic uncertainties and extraction of the proton's weak charge
- Implications of the new precision measurement of the proton's weak charge

Outline

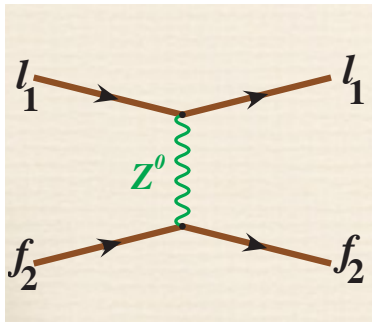
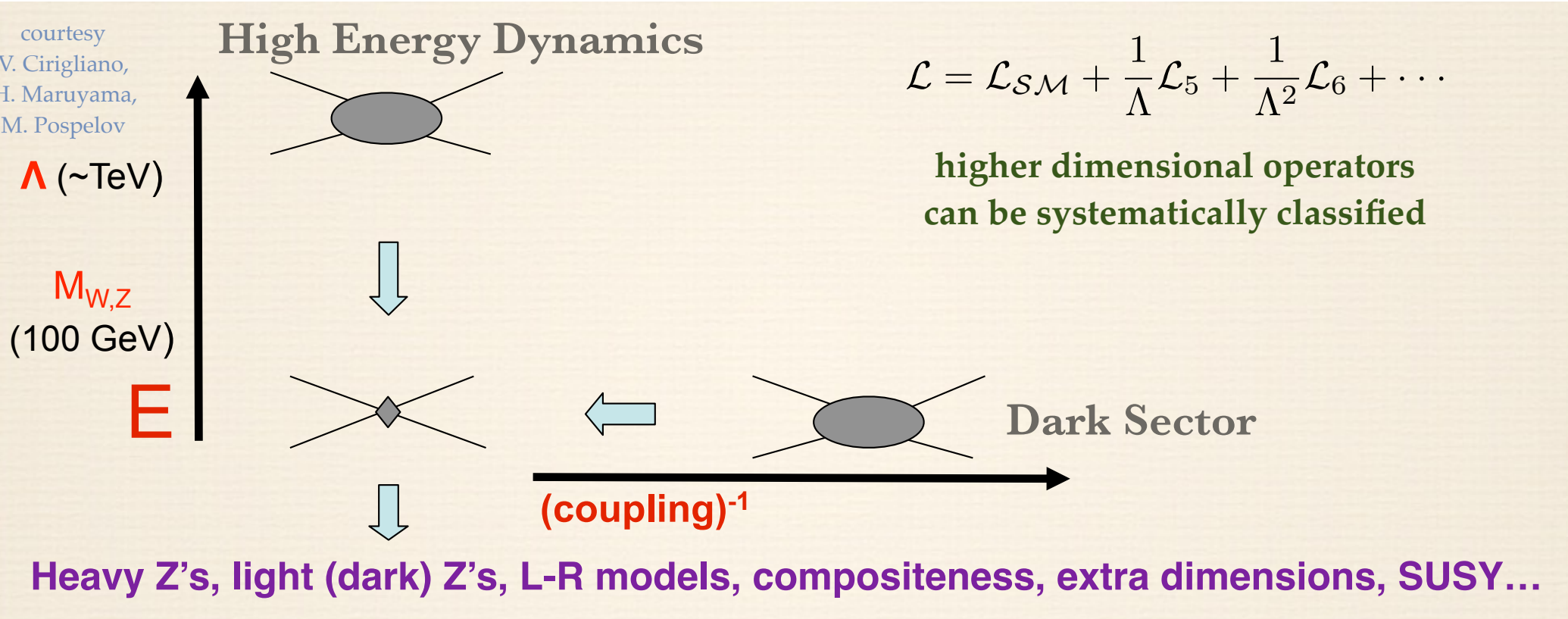
- Motivation and formalism
- Experiment: technical challenges and achievements
- Analysis: Key systematic uncertainties and extraction of the proton's weak charge
- Implications of the new precision measurement of the proton's weak charge

Standard Electroweak Model and Beyond

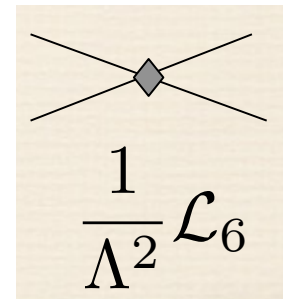
Standard EW Model = Renormalizable Gauge Theory

+ Spontaneous Symmetry Breaking

➔ believed to be incomplete



Q_{weak} sensitive to new neutral weak currents



The Hunt for New Physics

Two complementary approaches to searching for “New Physics”

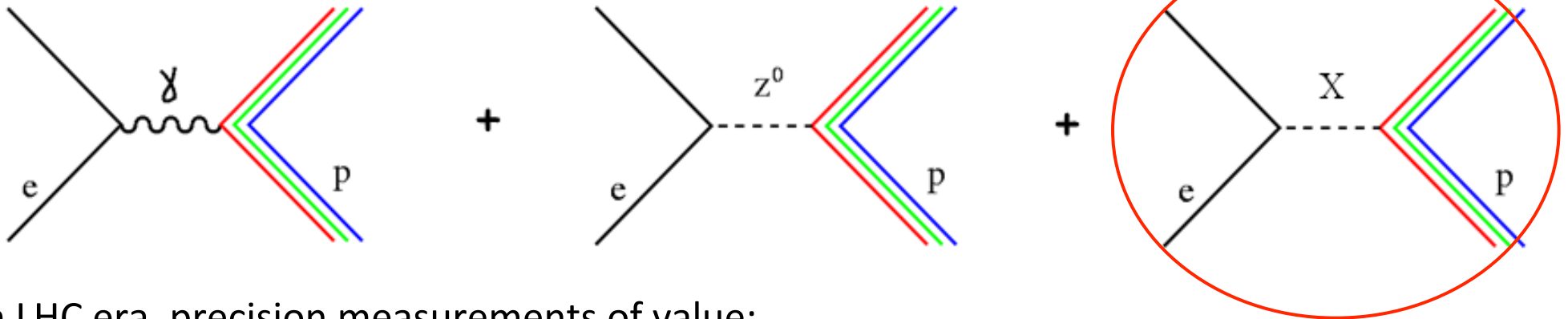
“Energy frontier” - like LHC

→ Make new particles (“X”) directly in high energy collisions



“Precision frontier” – weak charge, $g-2(\mu)$, etc.

→ Measure indirect effects of new particles (“X”) made virtually in low energy processes



In LHC era, precision measurements of value:

- If LHC sees “new physics”, precision measurements can help select among models
- If LHC sees no “new physics”, precision measurements are sensitive to some types of new physics unobservable at LHC

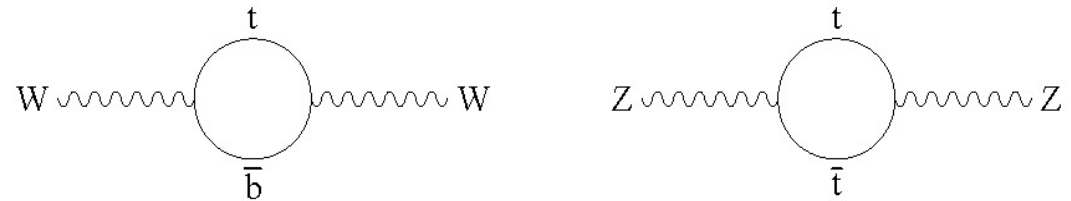
Historical Example: Top Quark

Past example of interplay between energy frontier and precision frontier

“Precision frontier”

Precision electroweak measurements (LEP at CERN and SLD at SLAC) were sensitive to “virtual top quarks” in loops

Prior to the direct top quark discovery, theorists predicted it would fall in a range from $145 \text{ GeV}/c^2 - 185 \text{ GeV}/c^2$



“Energy frontier”

Top quark was produced directly at Tevatron at Fermilab in 1995

Direct production at energy frontier



CDF 176.1 ± 6.6

DØ 172.1 ± 7.1

Average 174.3 ± 5.1

Indirect evidence at precision frontier



LEP1/SLD 170.7 ± 10.3

LEP1/SLD/ m_W/Γ_W 177.5 ± 9.3

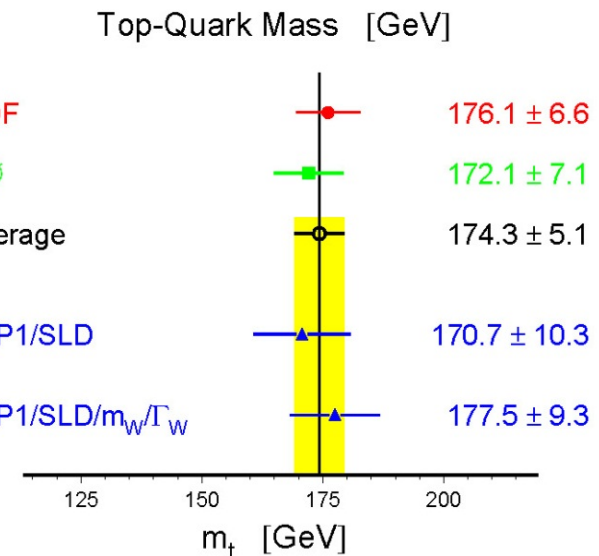
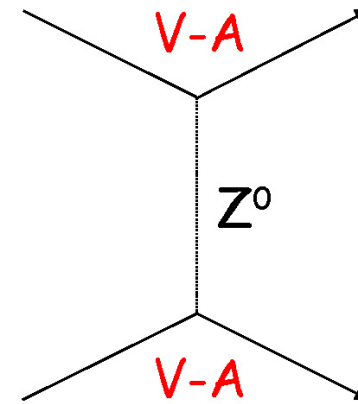


Figure 4. Measurements of the top quark mass at Fermilab (CDF and DØ) and indirect predictions from precision measurements (LEP1, SLD and M_W).³

Standard Model Weak Neutral Current Couplings

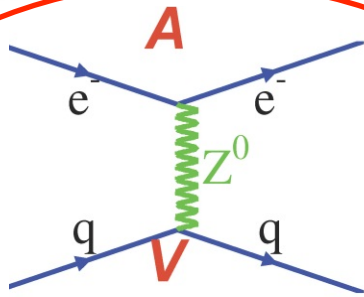
The Standard Model prescribes the couplings of the fundamental fermions to the Z boson:

fermions	$g_A^f = I_3$	$g_V^f = I_3 - 2Q \sin^2 \theta_W$
ν_e, ν_μ	$\frac{1}{2}$	$\frac{1}{2}$
e^-, μ^-	$-\frac{1}{2}$	$-\frac{1}{2} + 2\sin^2 \theta_W$
u, c	$\frac{1}{2}$	$\frac{1}{2} - \frac{4}{3}\sin^2 \theta_W$
d, s	$-\frac{1}{2}$	$-\frac{1}{2} + \frac{2}{3}\sin^2 \theta_W$



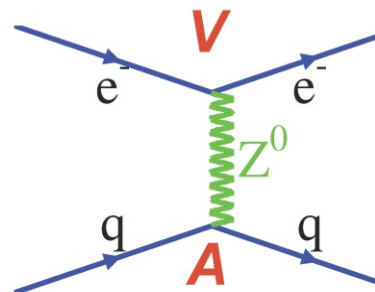
For low energy electroweak tests ($Q^2 \ll M_Z^2$), restrict to parity-violating e-q and e-e four-fermion contact interaction:

$$\mathcal{L}^{PV} = \frac{G_F}{\sqrt{2}} [\bar{e}\gamma^\mu \gamma_5 e (C_{1u} \bar{u}\gamma_\mu u + C_{1d} \bar{d}\gamma_\mu d) + \bar{e}\gamma^\mu e (C_{2u} \bar{u}\gamma_\mu \gamma_5 u + C_{2d} \bar{d}\gamma_\mu \gamma_5 d) + C_{ee} \bar{e}\gamma^\mu \gamma_5 e (\bar{e}\gamma_\mu e)]$$



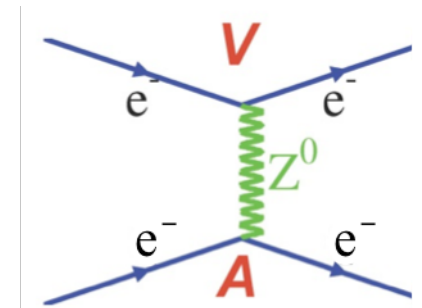
$$C_{1i} \equiv 2g_A^e g_V^i$$

quark vector: C_{1u}, C_{1d}



$$C_{2i} \equiv 2g_V^e g_A^i$$

quark axial-vector: C_{2u}, C_{2d}



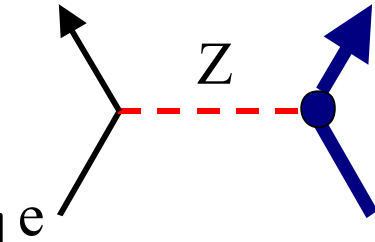
$$C_{ee} \equiv 2g_V^e g_A^e$$

electron: C_{ee}

C_{1u}, C_{1d}, C_{ee} : "Weak Charges": neutral current analog to the electric charges

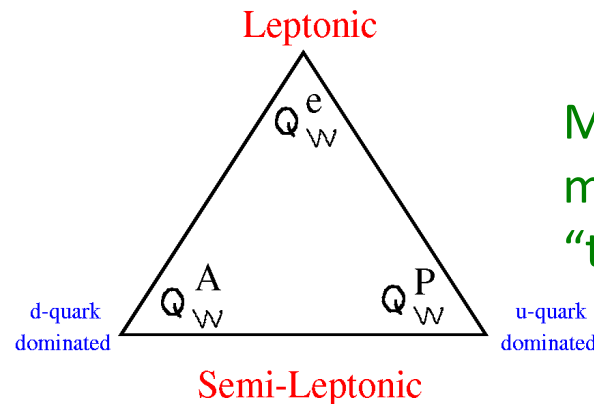
“Weak Charges” in Low Energy Neutral Current Tests

C_{1u}, C_{1d}, C_{ee} : “Weak Charges”: neutral current analog to the electric charges



Electron’s weak charge: $Q_W^e \equiv -2C_{ee} = -(1 - 4\sin^2 \theta_W)$
 parity-violating Møller scattering $\vec{e} + e \rightarrow e + e$

- **published: SLAC E158 ~ 13% on Q_W^e**



Most precise low energy measurements define a weak charge “triad” (M. Ramsey-Musolf)

“Neutron’s weak charge”:

$$Q_W^A(Z, N) \equiv -2[C_{1u}(2Z + N) + C_{1d}(Z + 2N)]$$

$$\approx Z(1 - 4\sin^2 \theta_W) - N(1) \approx -N$$

Atomic parity violation

- **published: ^{133}Cs ~ 0.6% on Q_W^A**

Proton’s weak charge:

$$Q_W^p \equiv -2[2C_{1u} + C_{1d}] = (1 - 4\sin^2 \theta_W)$$

parity-violating elastic ep scattering

$$\vec{e} + p \rightarrow e + p$$

- **Results today: JLab Qweak ~ 6% on Q_W^p**

Q_W^e and Q_W^p are suppressed in Standard Model \rightarrow increased sensitivity to new physics.
 ie. 6% on $Q_W^p=0.0708$ sensitive to **new neutral current amplitudes as weak as $\sim 4 \times 10^{-3} G_F$**

Parity-Violating Asymmetry for the Q_{weak} Experiment

$$\rightarrow e^- + p \rightarrow e^- + p$$

$$A = \frac{\sigma_R - \sigma_L}{\sigma_R + \sigma_L} \propto \frac{\langle \gamma | \dots | Z \rangle}{|\langle \gamma | \dots | \rangle|^2}$$

The Q_{weak} experiment at JLAB determines the proton's weak charge by measuring the parity-violating asymmetry in elastic scattering of longitudinally polarized electrons on proton.

$$A_{\text{PV}} = \frac{2M_{\text{NC}}}{M_{\text{EM}}} = \left[\frac{-G_F Q^2}{4\sqrt{2}\pi\alpha} \right] \left[\frac{\varepsilon G_E^\gamma G_E^Z + \tau G_M^\gamma G_M^Z - (1 - 4\sin^2\theta_W)\varepsilon' G_M^\gamma G_A^Z}{\varepsilon(G_E^\gamma)^2 + \tau(G_M^\gamma)^2} \right]$$

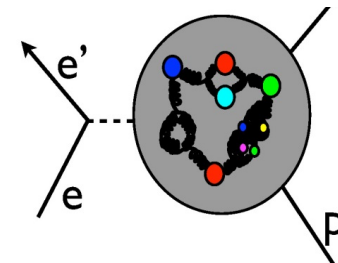
At forward scattering angles and low 4-momentum transfer:

$$A \equiv \frac{d\sigma_+ - d\sigma_-}{d\sigma_+ + d\sigma_-} \xrightarrow[\theta \rightarrow 0]{Q^2 \rightarrow 0} \left[\frac{-G_F}{4\pi\alpha\sqrt{2}} \right] \left[Q^2 Q_{\text{weak}}^p + Q^4 B(Q^2) \right]$$

proton's weak charge:
 $Q_{\text{weak}}^p = 1 - 4\sin^2\theta_W$ at tree level

“Form factor” term due to finite proton size – hadronic structure ($\sim 30\%$ for Q_{weak}) – determined well by existing PVES high Q^2 data

By running at a small value of Q^2 (small beam energy, small scattering angle) we minimize our sensitivity to the effects of the proton's detailed spatial structure.



Outline

- Motivation and formalism
- **Experiment: technical challenges and achievements**
- Analysis: Key systematic uncertainties and extraction of the proton's weak charge
- Implications of the new precision measurement of the proton's weak charge

Parity-Violating Electron Scattering Experiments – A Brief History

Pioneering (1978) early SM test

SLAC E122 PVDIS – Prescott *et al.*

$A = -152$ ppm

Strange Form Factors

(1998 – 2009)

SAMPLE, G0, A4, HAPPEX

$A \sim 1 - 50$ ppm

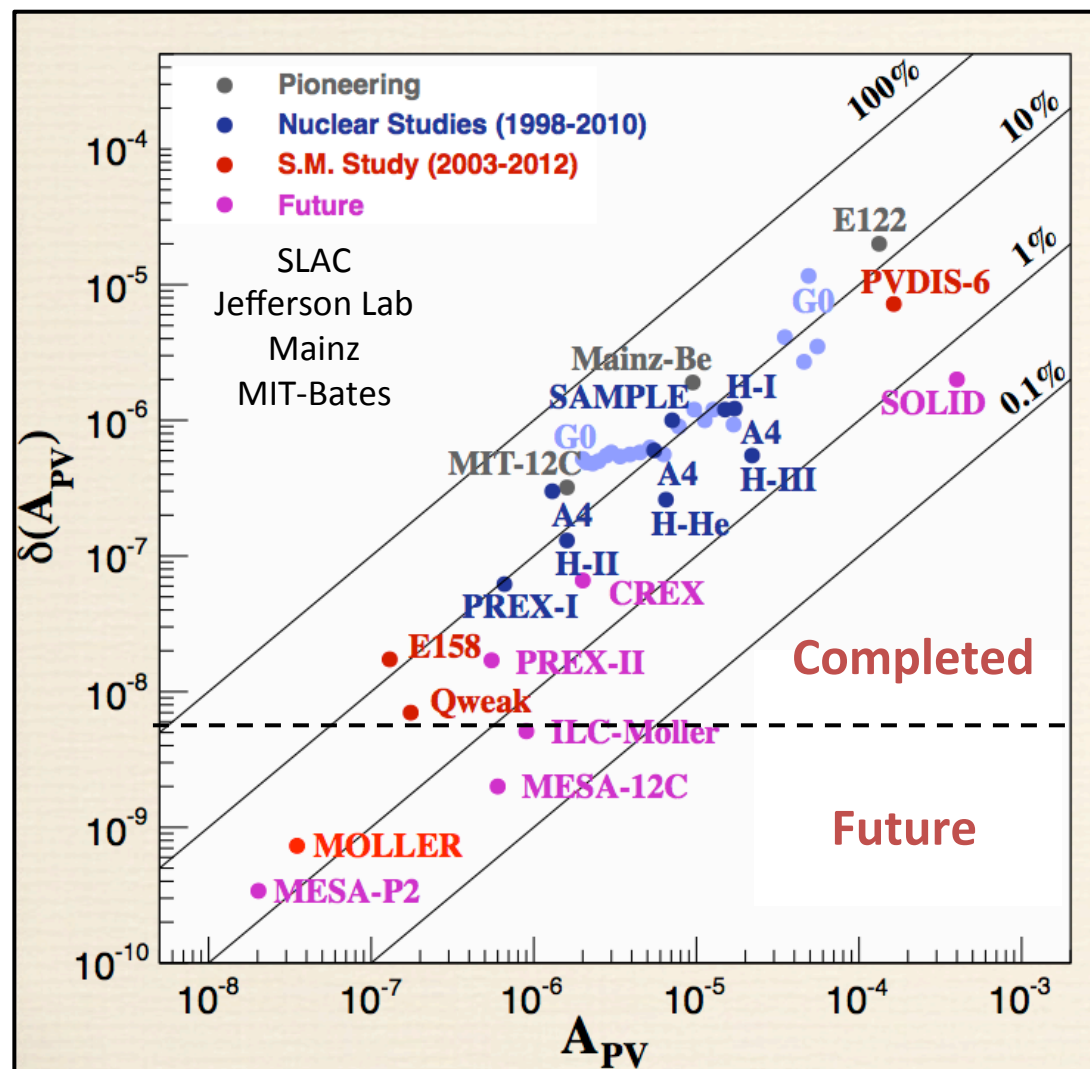
Standard Model Tests

(2003 – present)

SLAC E158 Moller: $A = -131$ ppb

JLAB Q_{weak} : $A \sim -230$ ppb, $\Delta A = 9$ ppb,

$\Delta A/A = 4\%$



Qweak Technical Challenges

$$A_{ep} = \frac{A_{meas} - A_{false}}{P_{beam}} - f_{back} A_{back} \quad (\text{for } f_{back} \ll 1)$$

Statistics on A_{meas}

- Small counting statistics error requires →
 - reliable high polarization, high current polarized source (**record 180 μA , 89% polarized beam delivered routinely for Qweak**)
 - high power cryogenic LH_2 target (**Qweak: world's highest power (3 kW), lowest density fluctuation target**)
 - large acceptance spectrometer and high count rate detectors/electronics

while minimizing contributions of random noise from

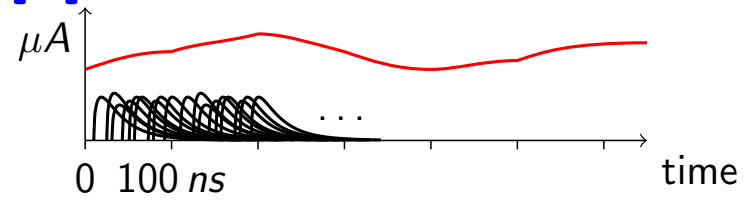
- target density fluctuations
- electronics noise (in integrating mode)

Systematics:

- Minimize helicity-correlated beam properties (A_{false}) (**much experience at Jlab**)
- Capability to isolate elastic scattering from other background processes (dilution factor f_{back} , background asymmetry A_{back})
- High precision electron beam polarimetry (P_{beam}) (**new Compton polarimeter in Hall C**)
- Precision Q^2 determination ($A_{ep} \propto Q^2$)

Qweak Experimental Apparatus

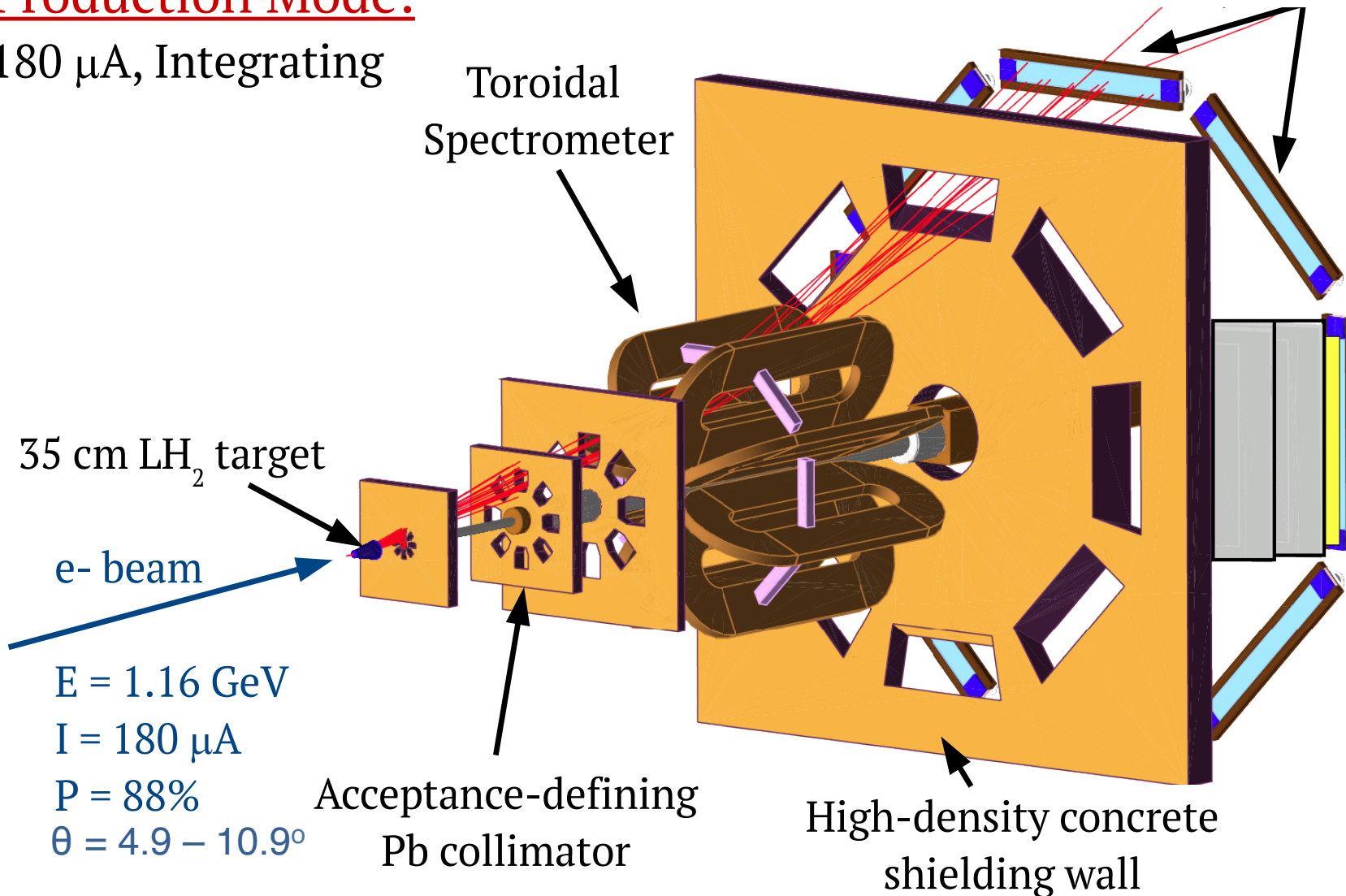
Production: ~ 800 MHz rates
must integrate PMT current



Quartz Bar Detectors

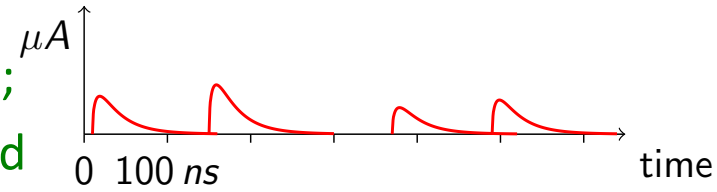
Production Mode:

180 μA , Integrating



Qweak Experimental Apparatus

Tracking (event) mode: low rate;
each event individually registered



Quartz Bar Detectors

Production Mode:

180 μA , Integrating

Tracking Mode:

50 pA, Counting
(Q^2 Systematics)

35 cm LH_2 target

e- beam

$E = 1.16 \text{ GeV}$

$I = 180 \mu\text{A}$

$P = 88\%$

$\theta = 4.9 - 10.9^\circ$

Toroidal Spectrometer

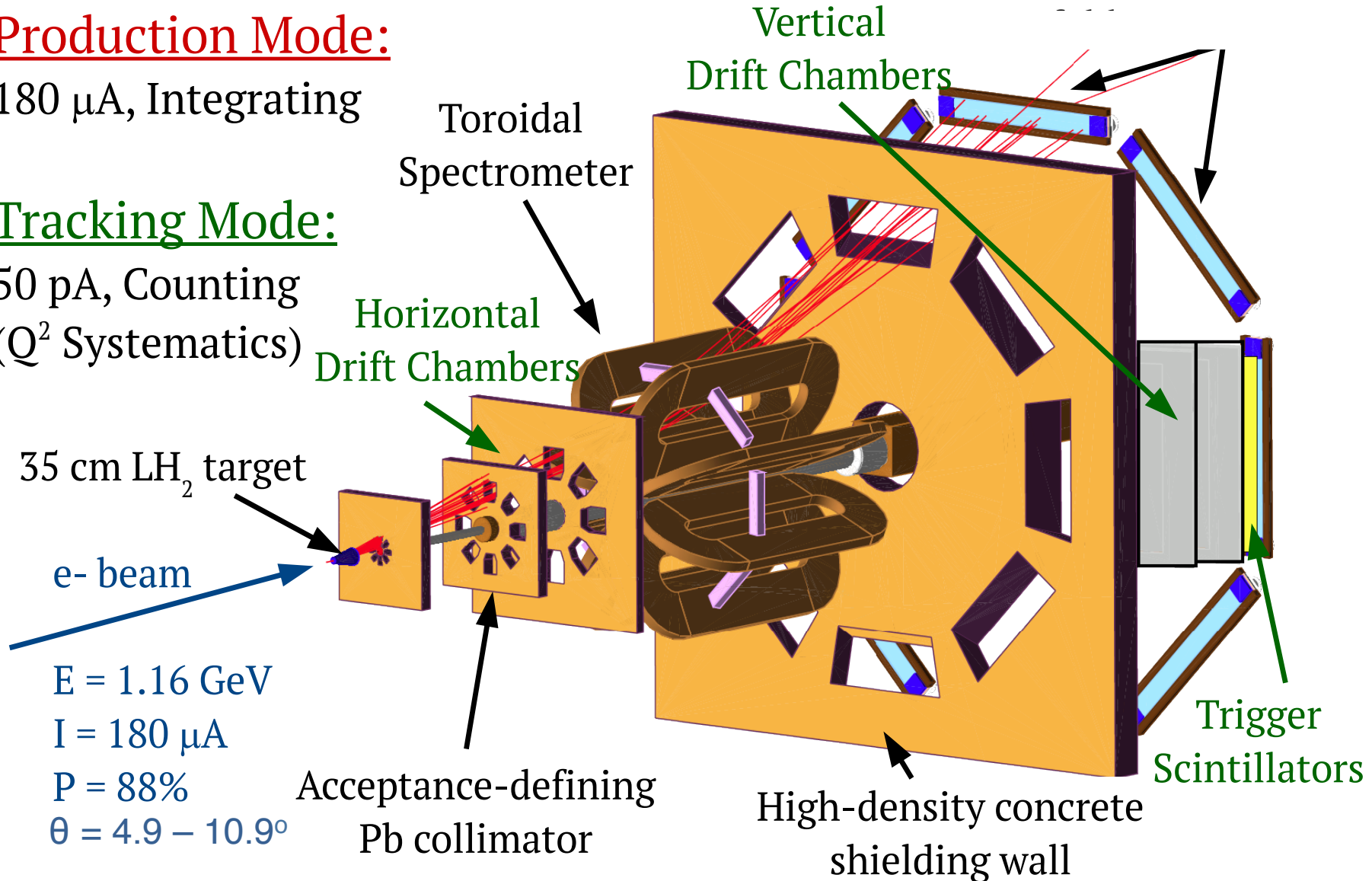
Horizontal Drift Chambers

Vertical Drift Chambers

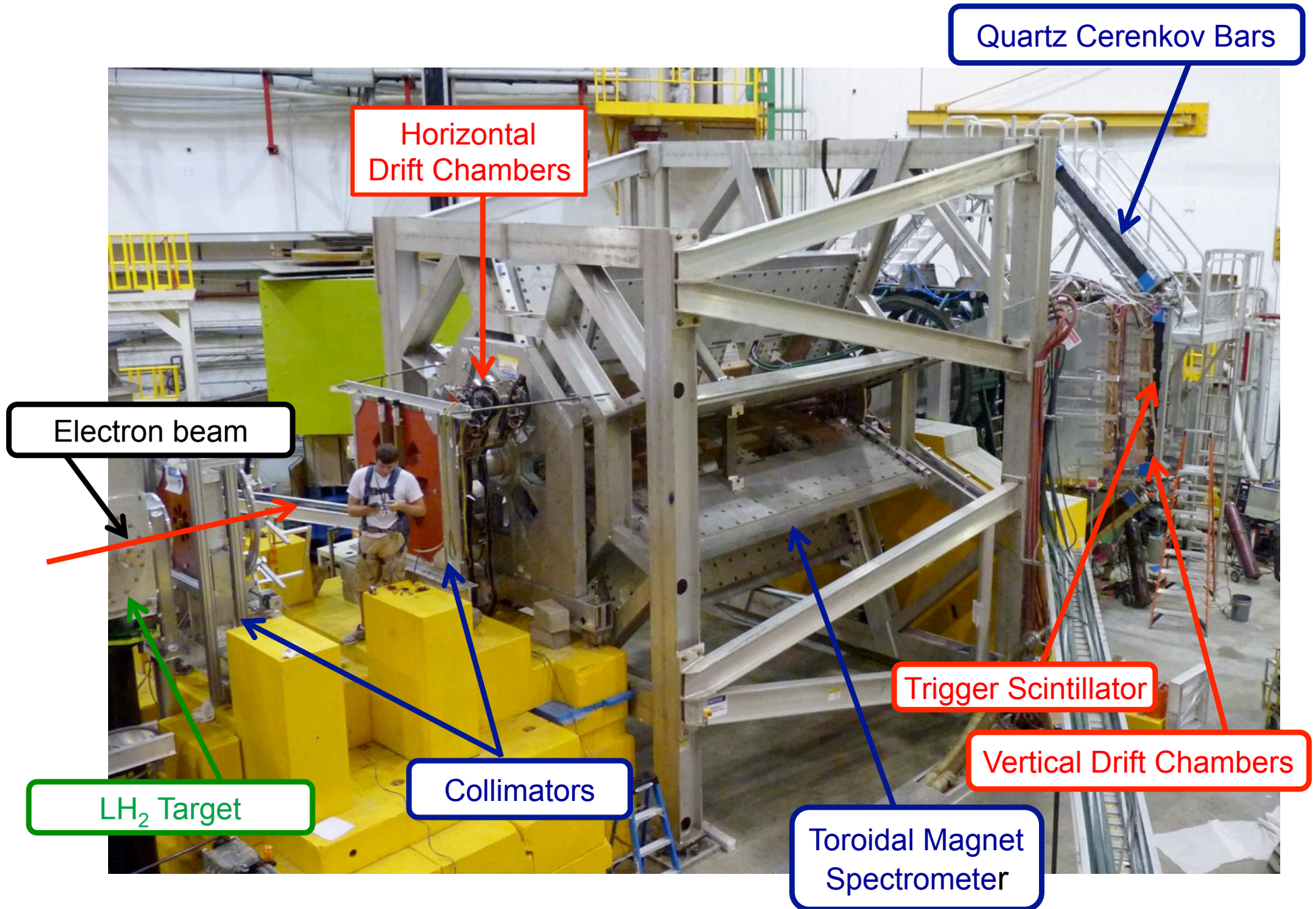
Acceptance-defining Pb collimator

High-density concrete shielding wall

Trigger Scintillators



Qweak Apparatus During Installation



Experimental Technique to Isolate/Measure PV Signal

The entire accelerator complex is our apparatus

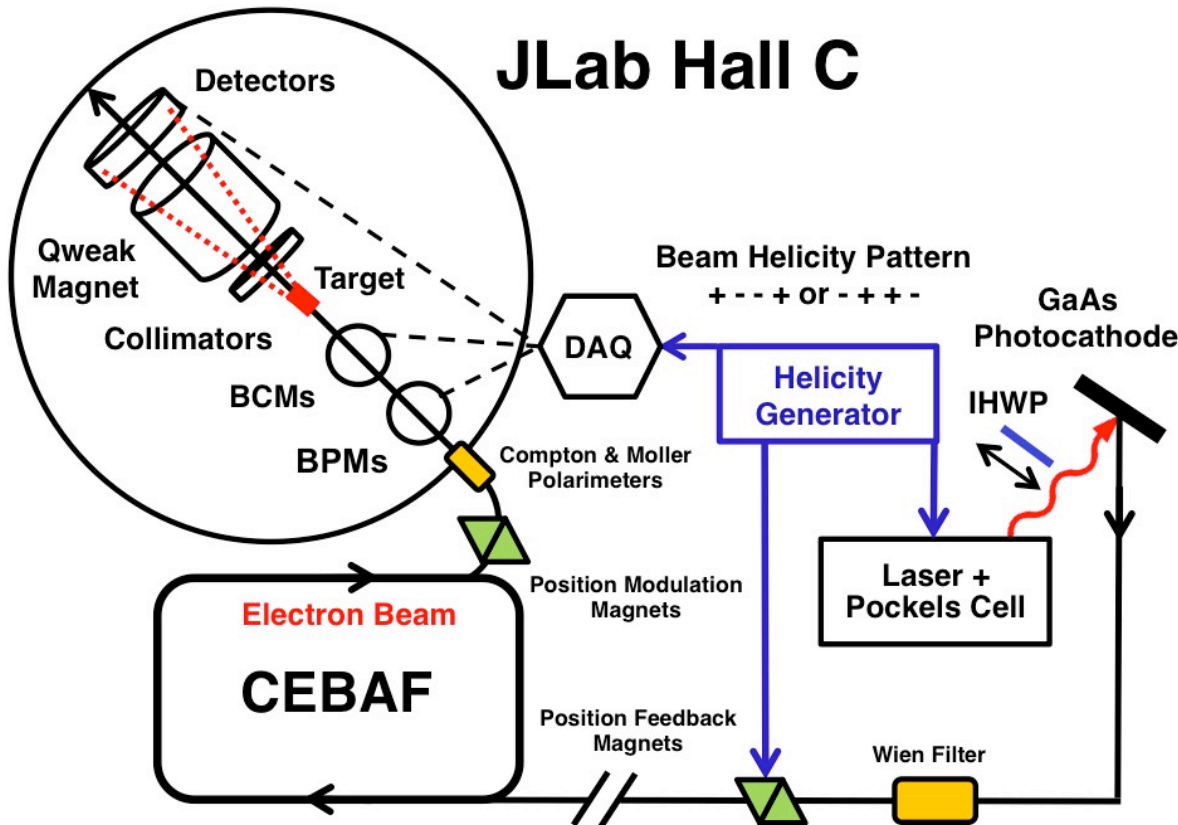
Multiple ways of reversing electron beam helicity are essential.

Rapid pseudo-random reversal (varying HV on Pockels cell) – 960 Hz – rejects LH₂ target density fluctuations

“Slow reversals”

Reverse electron beam helicity without changing Pockels cell HV

- **IHWP (insertable half wave plate) at ~ 8 hour intervals**
Purely mechanical
- **“Double Wien” spin manipulator at monthly intervals**
- **g-2 spin flip**
Changed to 2 pass (from 1 pass) once during run



Parity-Violating Electron Scattering Method

How do we take the bulk of our data? Pretty simple actually...

- Integrate the light signal in the Cerenkov detectors, sum them, and record the value every 1 msec

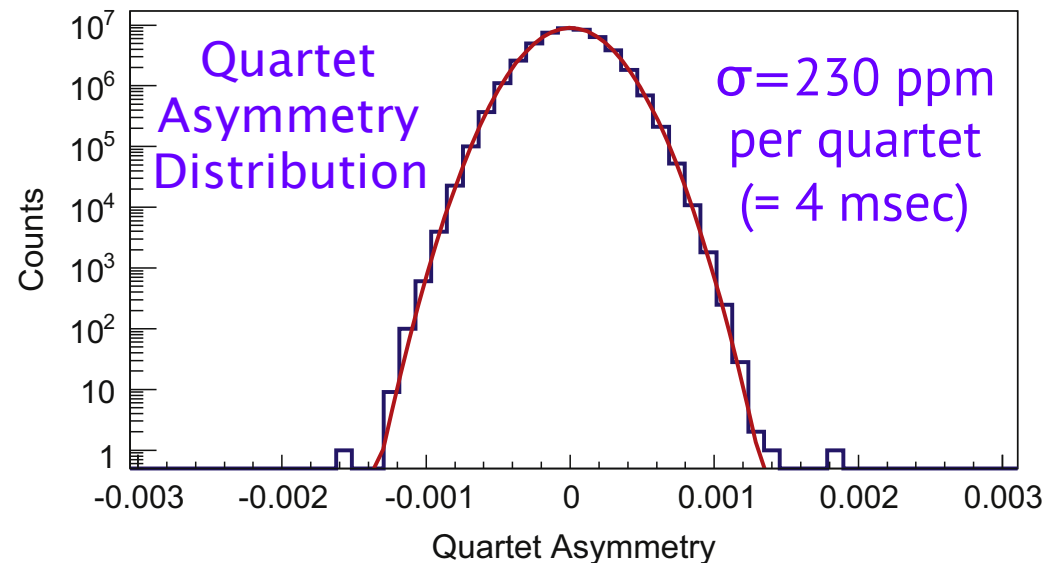
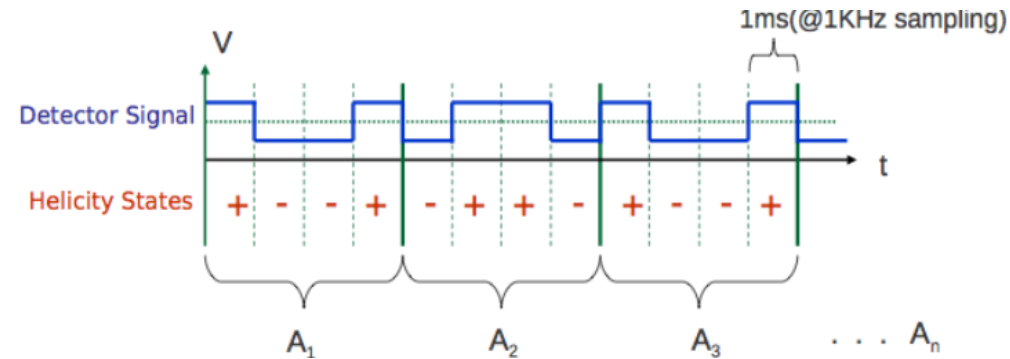
- “Normalize” the integrated signal (S) to the amount of charge (Q) in the beam

$$Y = \frac{S}{Q}$$

- Flip the electron beam helicity and form the asymmetry from four adjacent data samples:

$$A_{PV} = \frac{Y^+ - Y^-}{Y^+ + Y^-}$$

- Repeat 2 billion times! (2200 hours of data-taking) to get desired statistical error



LH2 statistical width (per quartet):

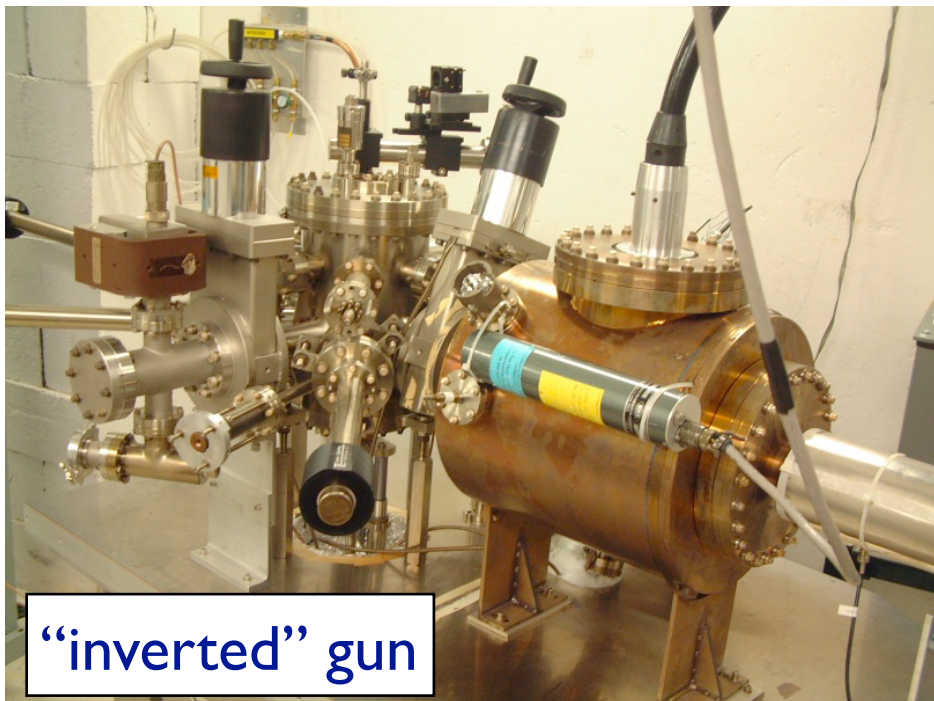
- Counting statistics: 200 ppm
- Main detector resolution: 92 ppm
- Target noise/boiling: 55 ppm
- BCM Resolution: 43 ppm
- Electronic noise: 3 ppm

Polarized source

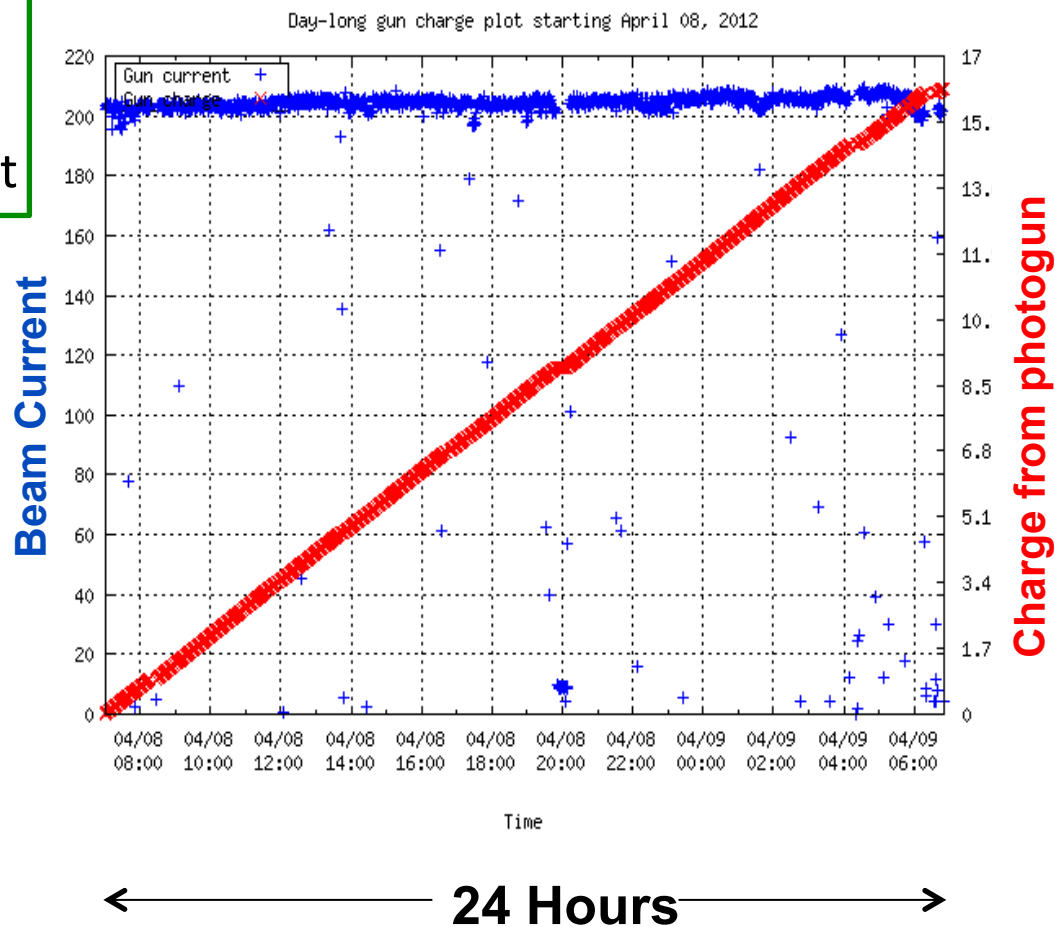
Q_{weak}: Polarized source routinely delivered 180 μ A at \sim 89% polarization for several months

New “inverted” gun

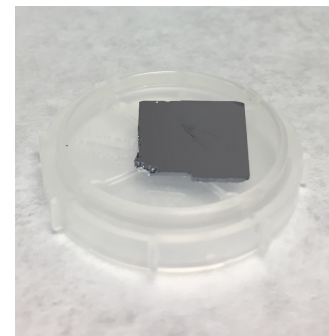
- 130 kV extraction: increase cathode lifetime, decrease space charge blowup for high current



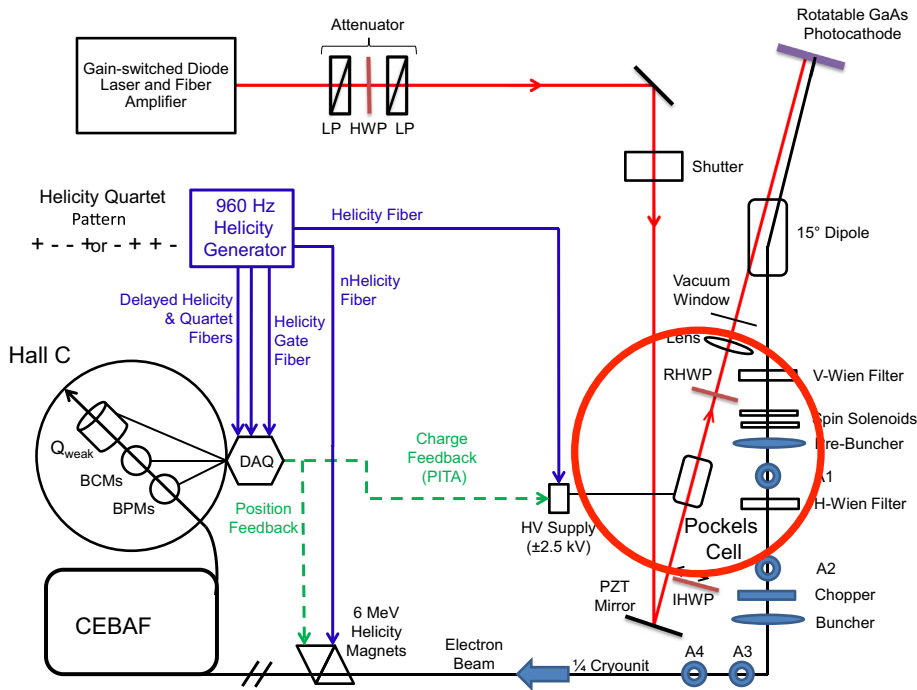
Record beam delivery during 24 hours of Qweak (2012)



Officially SLSP-5247-1
but known as the
“Qweak photocathode”
- a great performer!



Beam Properties



Minimization of helicity-correlated beam parameters is important to reduce false asymmetries

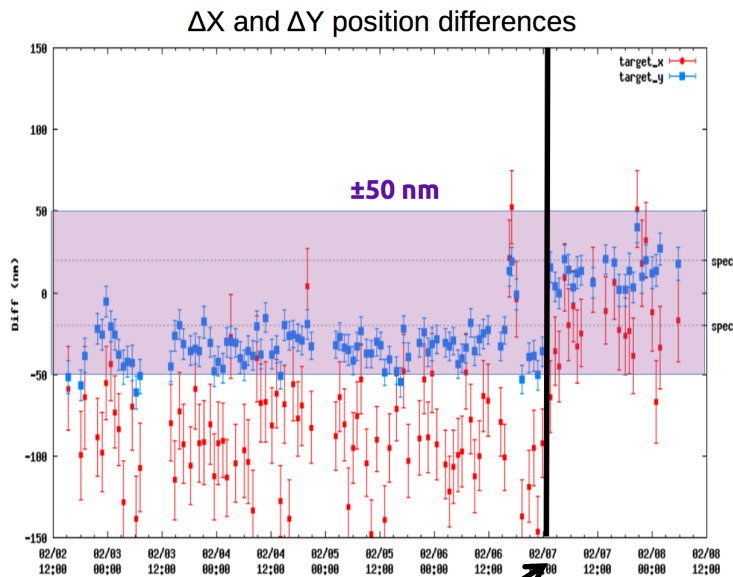
Intensity: active feedback (~60 sec. scale) on Pockels cell high voltage (~ 10 ppb)

Position:

- Careful alignment of Pockels cell and rotating half wave plate (RHWP) in source essential (smallest position differences after photocathode yet seen at Jlab)
- Did not (generally) benefit from “kinematic damping” $x, x' \propto \sqrt{p/p_0}$
- Active feedback with “helicity-corrector” magnets in 5 MeV region during Run 2

Results:

- Injector: ~ 50 nm
- Hall: ~ 100 nm
- Reversals: ~ 10 nm
- Feedback: ~1-2 nm

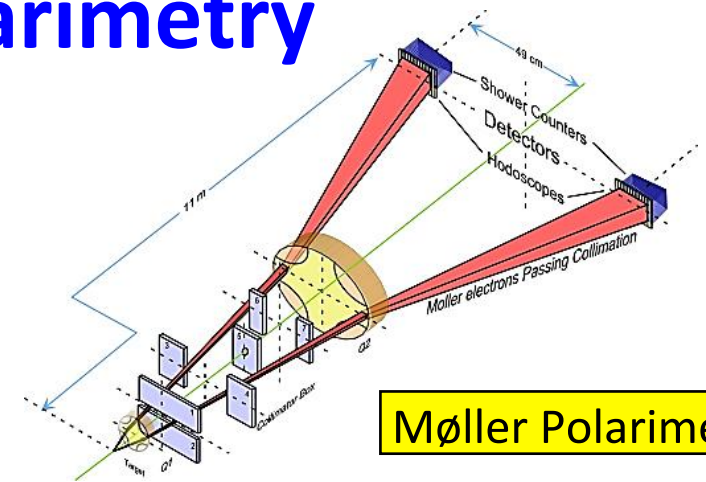


Helicity magnets turned on

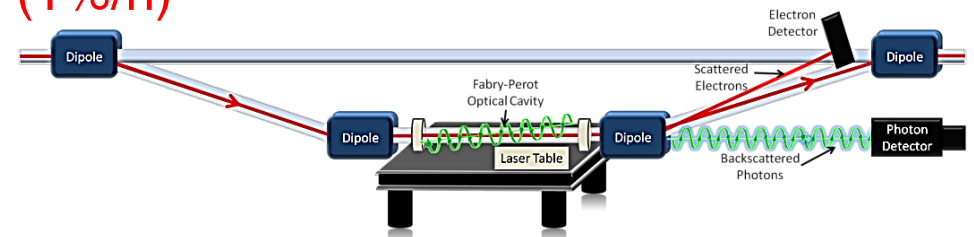
Precision Beam Polarimetry

Strategy: use 2 independent polarimeters

- Use existing <1% Hall C Møller polarimeter:
 - Low beam currents, invasive
 - Known analyzing power provided by polarized “saturated” Fe foil in a 3.5 T field.
- Compton (photon & electron) polarimeter (1%/h)
 - Continuous, non-invasive
 - Known analyzing power provided by circularly-polarized laser

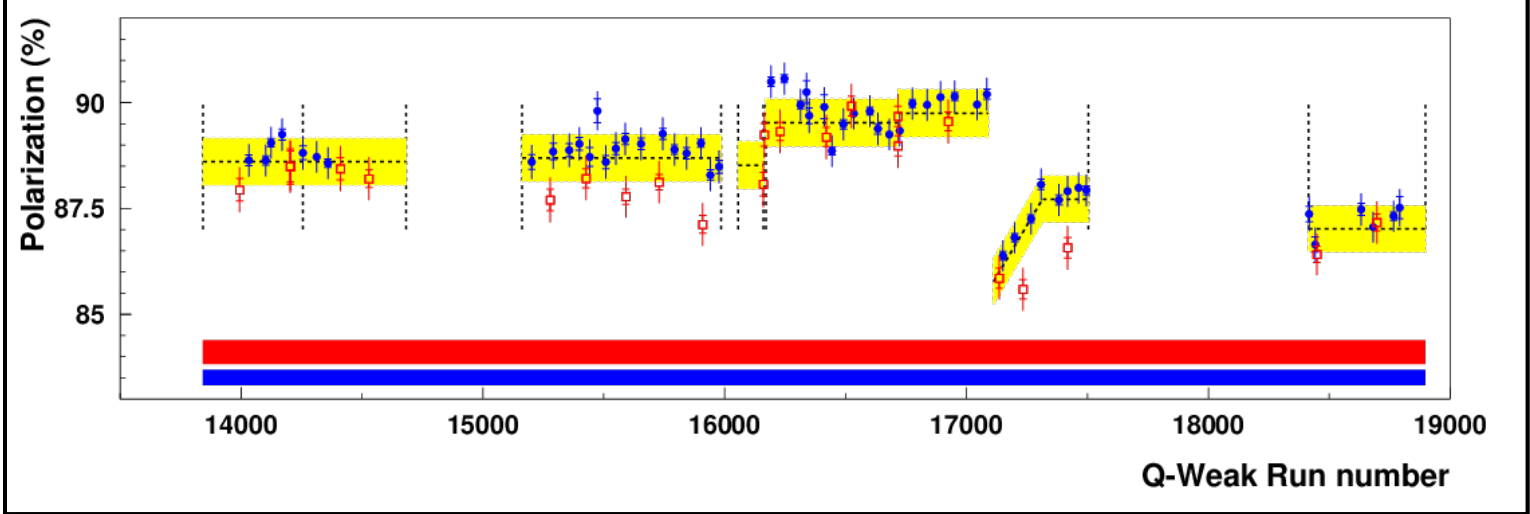


Møller Polarimeter



Compton Polarimeter

Run 2 Compton (blue circle) and Moller (red square) measurements versus data run #



~ 0.6% precision achieved during Run 2

Publications:

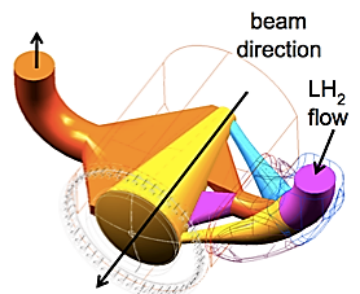
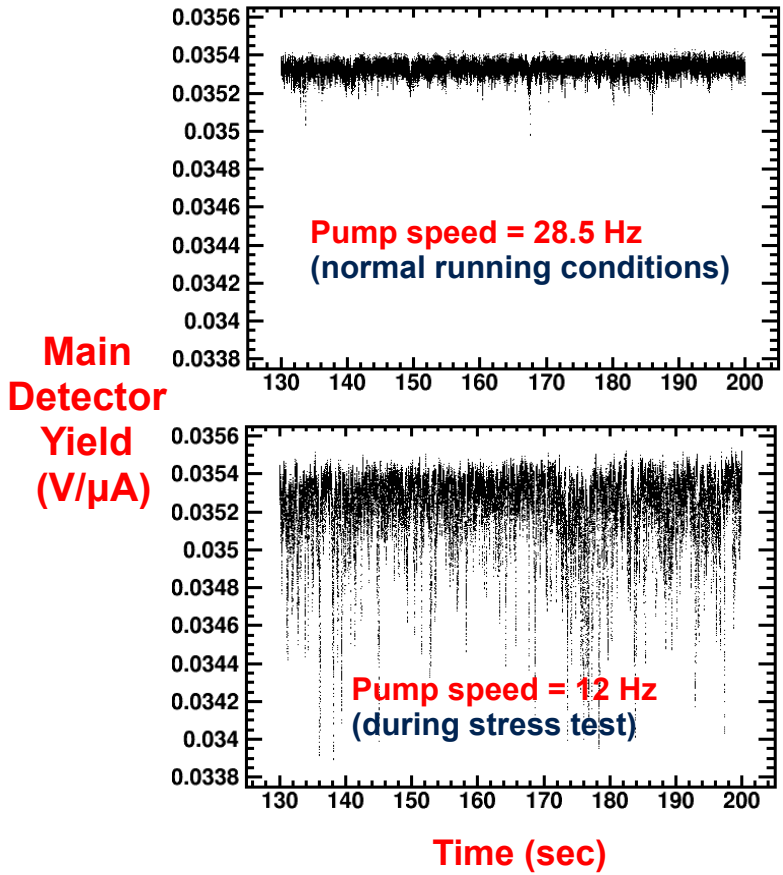
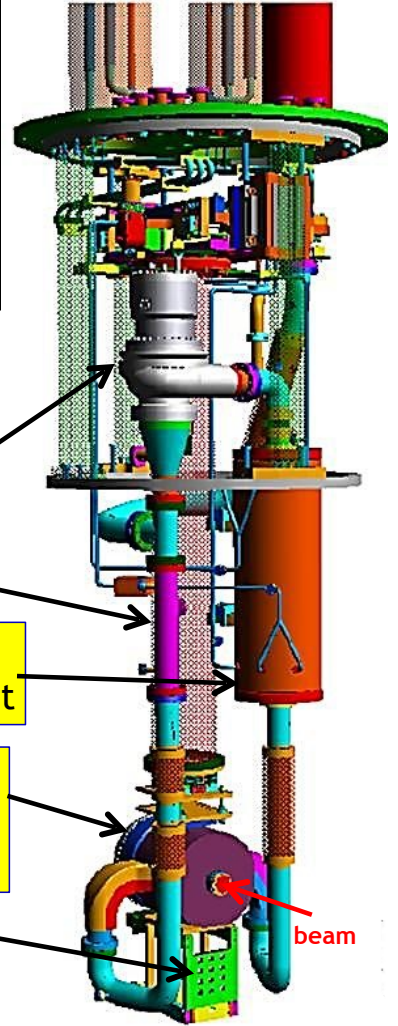
- Phys. Rev X 6, 011013 (2016) – Compton with diamond detectors
- Phys. Lett. B 766, 339 (2017) – Moller/ Compton comparison

Liquid Hydrogen Target

- World's highest power (~ 3 kW) and lowest noise cryotarget
- Used computational fluid dynamics (CFD)
- Designed to minimize contribution to random noise from target density fluctuations – “boiling”

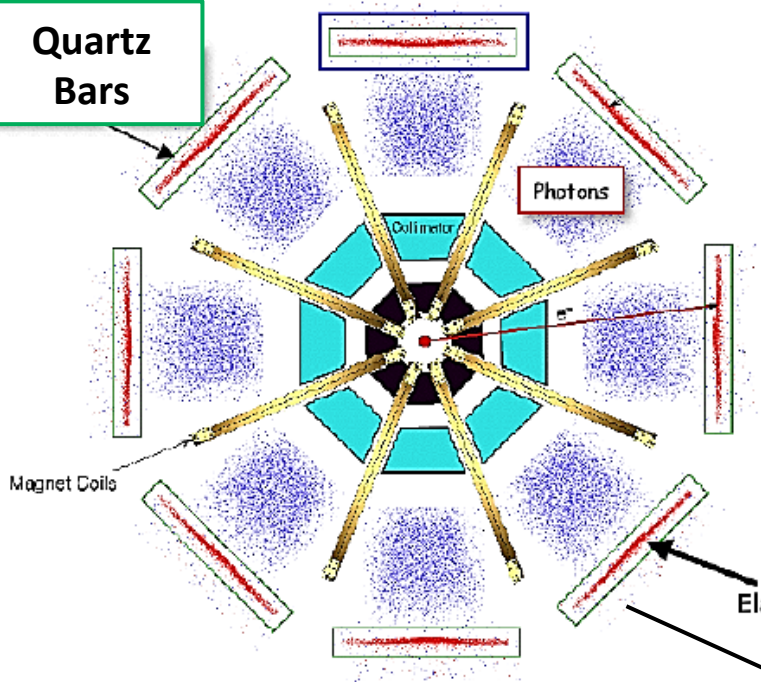
Achieved! ~ 50 ppm < 230 ppm counting statistics noise

$I_{\text{Beam}} = 180 \mu\text{A}$
 $L = 35 \text{ cm (4\% } X_0)$
 $P_{\text{beam}} = 2.2 \text{ kW}$
 $A_{\text{spot}} = 4 \times 4 \text{ mm}^2$
 $V = 57 \text{ liters}$
 $T = 20.00 \text{ K}$
 $P \sim 220 \text{ kPa}$

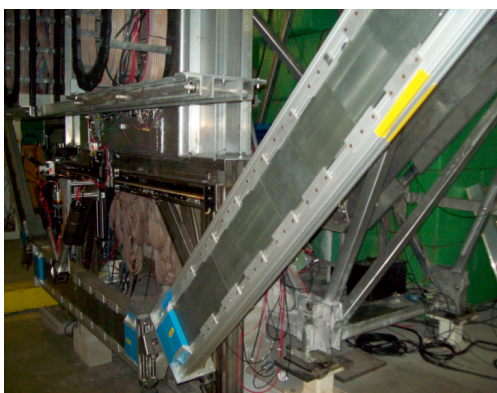
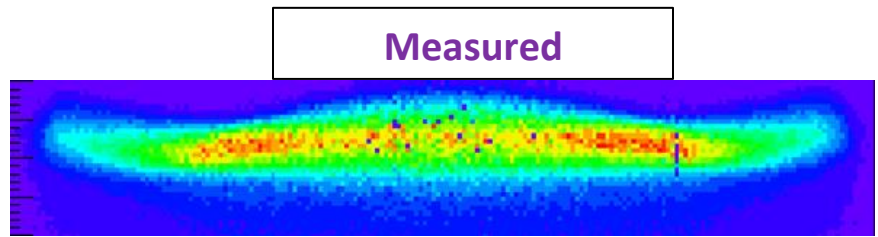


Q_{weak} Main Cerenkov Detector and Spectrometer

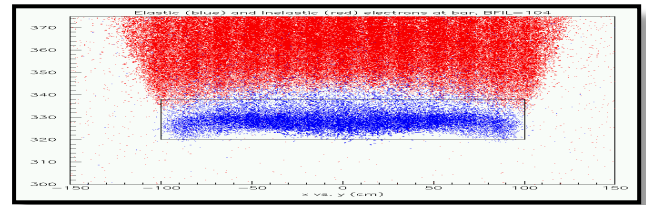
Azimuthal symmetry maximizes rate and decreases sensitivity to HC beam motion, transverse asymmetry.



- Main detector: Large array of eight Cerenkov radiator bars (each 200 cm x 18 cm x 1.25 cm)
- artificial fused silica for UV transmission, polished to 25 Angstroms (rms)
- **Spectrosil 2000: rad-hard, non-scintillating, low-luminescence**
- Two 5" PMTs per bar, S20 cathodes for high light levels
- Yield 100 pe's/track with 2 cm Pb pre-radiators
- Resolution (~10%) limited by shower fluctuations.



Toroidal Spectrometer Produces 8 Beam Spots
Each focus is ~2 meters long



Elastic focus – blue Inelastics - red

Outline

- Motivation and formalism
- Experiment: technical challenges and achievements
- **Analysis: Key systematic uncertainties and extraction of the proton's weak charge**
- Implications of the new precision measurement of the proton's weak charge

Q_{weak} Data-Taking Periods

Q_{weak} had ~ 1 calendar year of beam split into 3 running periods

Each period had its own “blinding factor” (additive offset in range ± 60 ppb) to avoid analysis bias:

- Run 0: January – February 2011 (only 4% of the total data)
(published in *Phys. Rev. Lett.* **111**, 141803 (2013))
- Run 1: February – May 2011
- Run 2: November 2011 – May 2012

From Measured Asymmetry to Physics Asymmetry

Correct **raw** asymmetry for measured false asymmetry effects to get **measured** asymmetry

$$A_{\text{msr}} = A_{\text{raw}} + A_T + A_L + A_{\text{BCM}} + A_{\text{BB}} + A_{\text{beam}} + A_{\text{bias}}$$

Correct **measured** asymmetry for polarization, backgrounds, acceptance, etc. to get **ep physics** asymmetry

$$A_{ep} = R_{\text{tot}} \frac{A_{\text{msr}}/P - \sum_{i=1,3,4} f_i A_i}{1 - \sum_{i=1}^4 f_i} \quad R_{\text{tot}} = R_{\text{RC}} R_{\text{Det}} R_{\text{Acc}} R_{Q^2}$$

Quantity	Run 1	Run 2
A_{raw}	-218.0* ±13.2 ppb	-164.0* ±7.3 ppb
A_T	0 ± 1.1 ppb	0 ± 0.7 ppb
A_L	1.3 ± 1.0 ppb	1.2 ± 0.9 ppb
A_{BCM}	0 ± 4.4 ppb	0 ± 2.1 ppb
A_{BB}	3.9 ± 4.5 ppb	-2.4 ± 1.1 ppb
A_{beam}	18.5 ± 4.1 ppb	0.0 ± 1.1 ppb
A_{bias}	4.3 ± 3.0 ppb	4.3 ± 3.0 ppb
P	87.7 ± 1.1%	88.71 ± 0.55%
f_1	2.471 ± 0.056%	2.516 ± 0.059%
A_1	1.514 ± 0.077 ppm	1.515 ± 0.077 ppm
f_2	0.193 ± 0.064%	0.193 ± 0.064%
f_3	0.12 ± 0.20%	0.06 ± 0.12%
A_3	-0.39 ± 0.16 ppm	-0.39 ± 0.16ppm
f_4	0.018 ± 0.004%	0.018 ± 0.004%
A_4	-3.0 ± 1.0 ppm	-3.0 ± 1.0ppm
R_{RC}	1.010 ± 0.005	1.010 ± 0.005
R_{Det}	0.9895 ± 0.0021	0.9895 ± 0.0021
R_{Acc}	0.977 ± 0.002	0.977 ± 0.002
R_{Q^2}	0.9927 ± 0.0056	1.0 ± 0.0056

→ ***Separate run 1,2 additive blinding offsets not yet removed from asymmetry!**

Several differences between Run 1 and 2:

- improved polarimetry in Run 2
- improved helicity-correlated beam corrections in Run 2
- improved beam charge monitor (BCM) readout electronics in Run 2
- different beam conditions in the two run periods

Tests our ability to do the corrections and uncertainty assessment properly

Most Significant Systematic Errors on A_{ep}

Period	Stat. Unc. (ppb)	Syst. Unc. (ppb)	Tot. Uncertainty (ppb)
Run 1	15.0	10.1	18.0
Run 2	8.3	5.6	10.0

Quantity	Run 1 error (ppb)	Run 1 fractional	Run 2 error (ppb)	Run 2 fractional
BCM Normalization: A_{BCM}	5.1	25%	2.3	17%
Beamline Background: A_{BB}	5.1	25%	1.2	5%
Beam Asymmetries: A_{beam}	4.7	22%	1.2	5%
Rescattering bias: A_{bias}	3.4	11%	3.4	37%
Beam Polarization: P	2.2	5%	1.2	4%
Target windows: A_{b1}	1.9	4%	1.9	12%
Kinematics: R_{Q^2}	1.2	2%	1.3	5%
Total of others	2.5	6%	2.2	15%
Combined in quadrature	10.1		5.6	

- Run 1 and 2 were both statistics limited
- Systematic error in Run 2 was significantly better than Run 1 due to known differences between the two periods

Dominant systematic errors were both expected and unexpected (as can happen when pushing the boundaries in precision):

Expected and planned for:

- Beam Asymmetries A_{beam}
- Aluminum target windows A_1

Unexpected but symmetry and auxiliary background detectors made them manageable

- Beamline background asymmetries A_{BB}
- Rescattering bias A_{bias}

Beam Asymmetries

$$A_{beam} = - \sum_{i=1}^5 \left(\frac{\partial A}{\partial \chi_i} \right) \Delta \chi_i$$

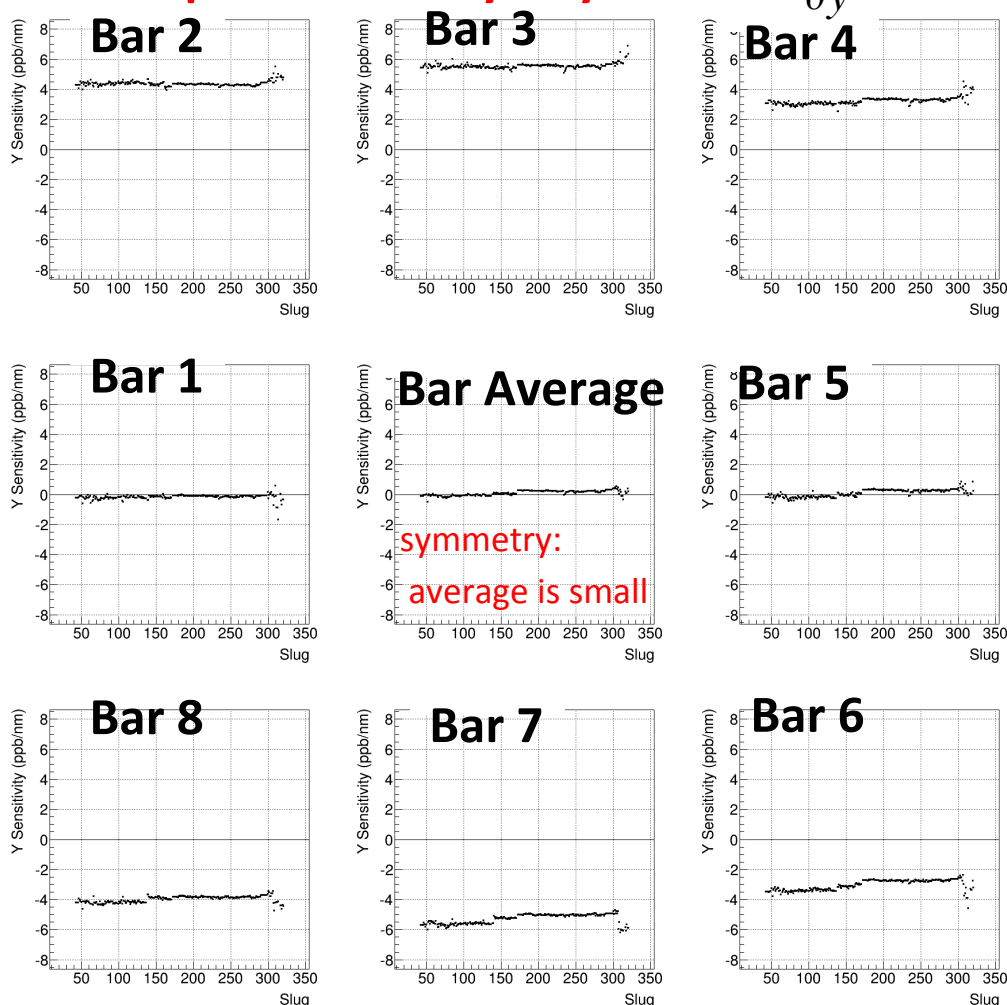
Correct for measured helicity-correlated beam properties using measured detector sensitivities (from deliberate modulation of position, angle, energy)

Helicity-correlated beam parameter differences for Run 1 and 2 and typical detector sensitivities.

Beam Parameter	Run 1 $\Delta \chi_i$	Run 2 $\Delta \chi_i$	Typical $\partial A / \partial \chi_i$
X	-3.5 ± 0.1 nm	-2.3 ± 0.1 nm	-2 ppb/nm
X'	-0.30 ± 0.01 nrad	-0.07 ± 0.01 nrad	50 ppb/nrad
Y	-7.5 ± 0.1 nm	0.8 ± 0.1 nm	< 0.2 ppb/nm
Y'	-0.07 ± 0.01 nrad	-0.04 ± 0.01 nrad	< 3 ppb/nrad
Energy	-1.69 ± 0.01 ppb	-0.12 ± 0.01 ppb	-6 ppb/ppb

- Helicity-correlated positions smaller in Run 2 than Run 1 (due to position feedback)
- Sensitivities: horizontal plane had larger symmetry breaking than vertical plane
- Interaction with accelerator fast feedback system led to multiple modulation modes- overdetermined set that allowed for uncertainty estimation

Example: sensitivity to y motion $\frac{\partial A}{\partial y}$



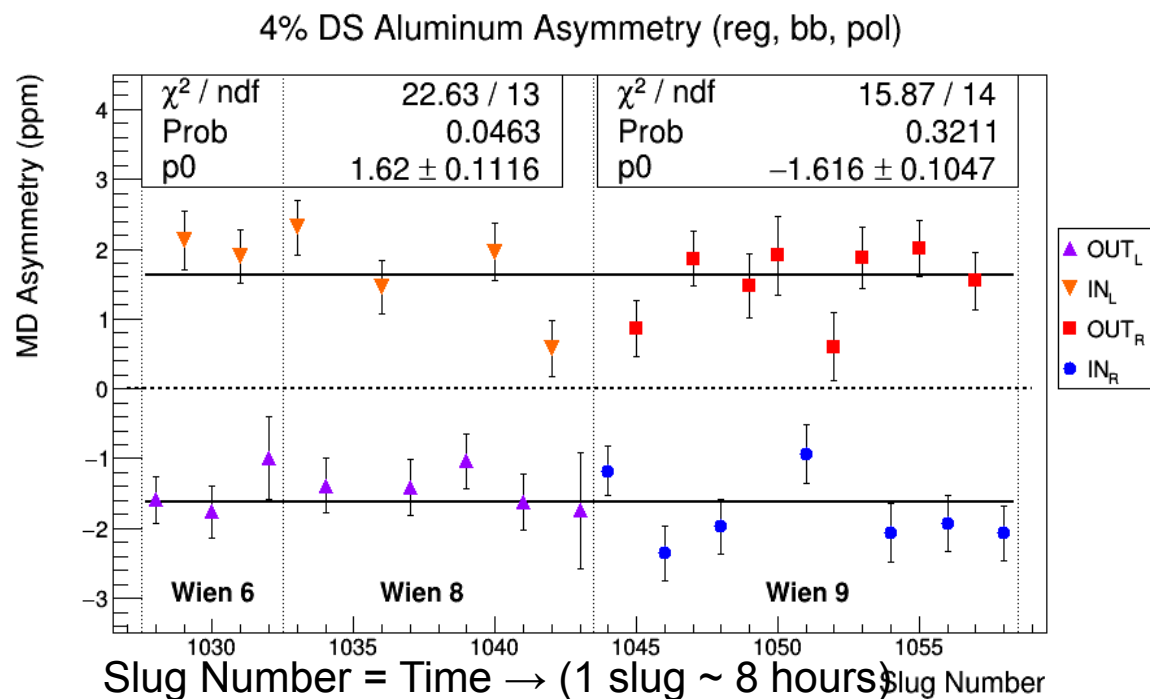
Run 1: $A_{beam} = 18.5 \pm 4.1$ ppb

Run 2: $A_{beam} = 0.0 \pm 1.1$ ppb

Aluminum Target Window Background

Dominant correction to the asymmetry: background from electrons that scatter from thin aluminum entrance and exit windows on hydrogen target

- **Dilution fraction (f_1):** directly measured with empty target
- **Asymmetry (A_1):** directly measured with dedicated beam time on thick “dummy” target of identical alloy to hydrogen target windows
- Corrections for effect of H_2 made using simulation and data-driven models of elastic and quasi-elastic scattering



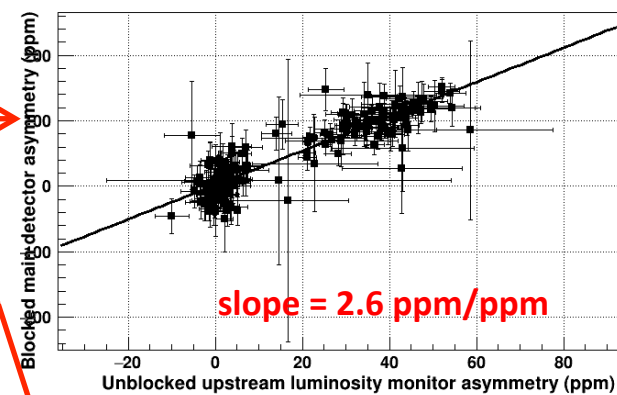
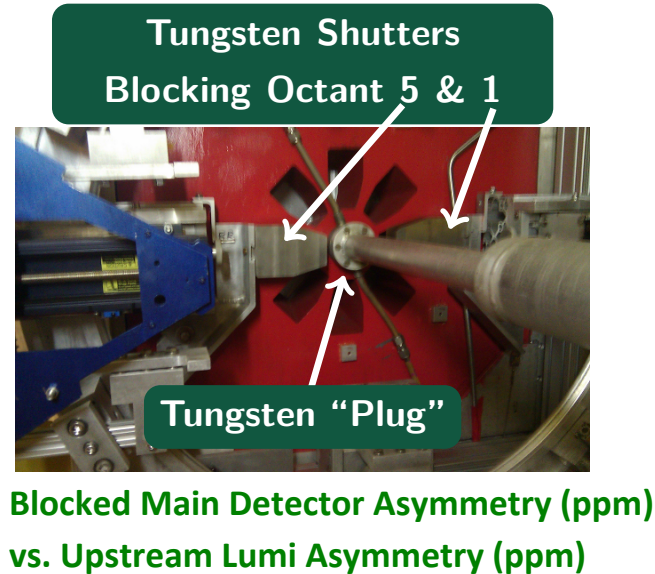
- Not sign corrected for slow reversals (IHWP and Wien); sign changing as expected
- Stat. unc. 4.7%, syst. unc. 1.4%
- Plan to extract the ^{27}Al asymmetry (theoretical support from Check Horowitz)

$$f_1 \sim 2.5\% \quad A_1 = 1515 \pm 77 \text{ ppb}$$

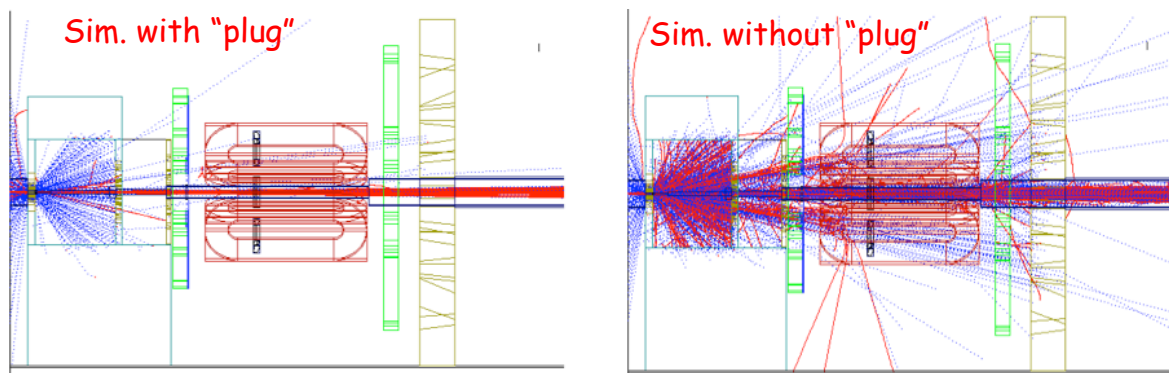
Resulting in a 38 ppb correction to the hydrogen asymmetry ($\sim 20\%$) – our largest correction

Beamline Background

- Background from electrons scattering on beamline or tungsten “plug” collimator; “plug” designed to keep it small
- **Dilution:** contributed small $f_2 = 0.19 \pm 0.06\%$ to main detector signal as directly measured by tungsten shutters
- **Unexpected:** the small beamline background had a **large asymmetry**, thought to be associated with large helicity-correlated charge or position asymmetries in the beam halo.
- **Dedicated background detectors** in various locations monitored this component and measured highly correlated asymmetries (**up to 20 ppm!**).
- **Asymmetry correction:** blocked octant study showed MD asymmetry highly correlated with background detectors; use measured correlation slope and background detector asymmetries to make correction

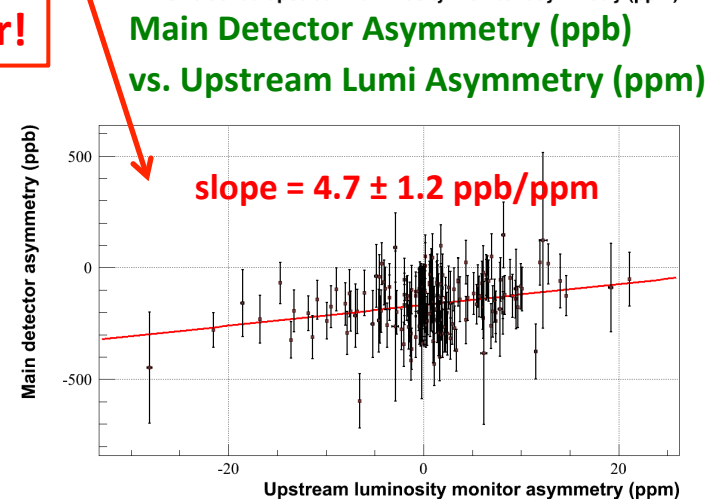


Run 1: $A_{BB} = 3.9 \pm 4.5$ ppb Run 2: $A_{BB} = -2.4 \pm 1.1$ ppb
Unexpected, but that’s what the background detectors were for!

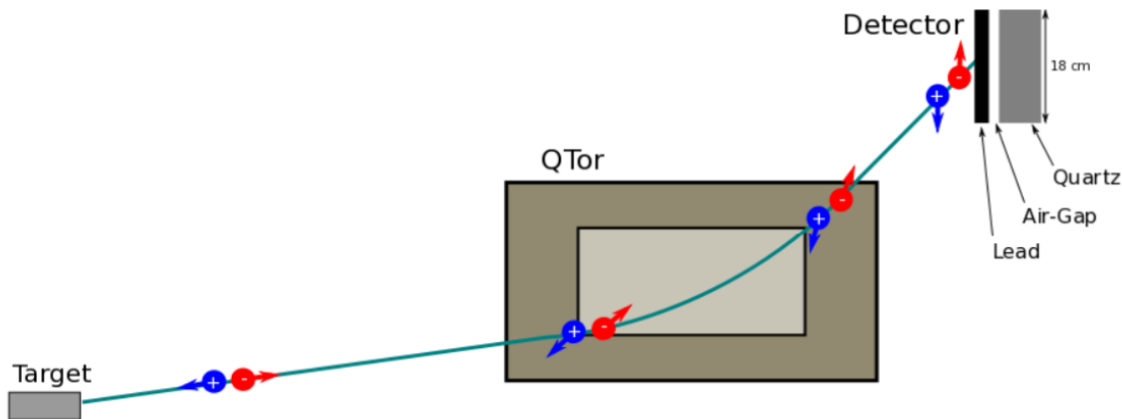


9/8/2017

Jefferson Lab Physics Seminar



Rescattering Bias, part 1



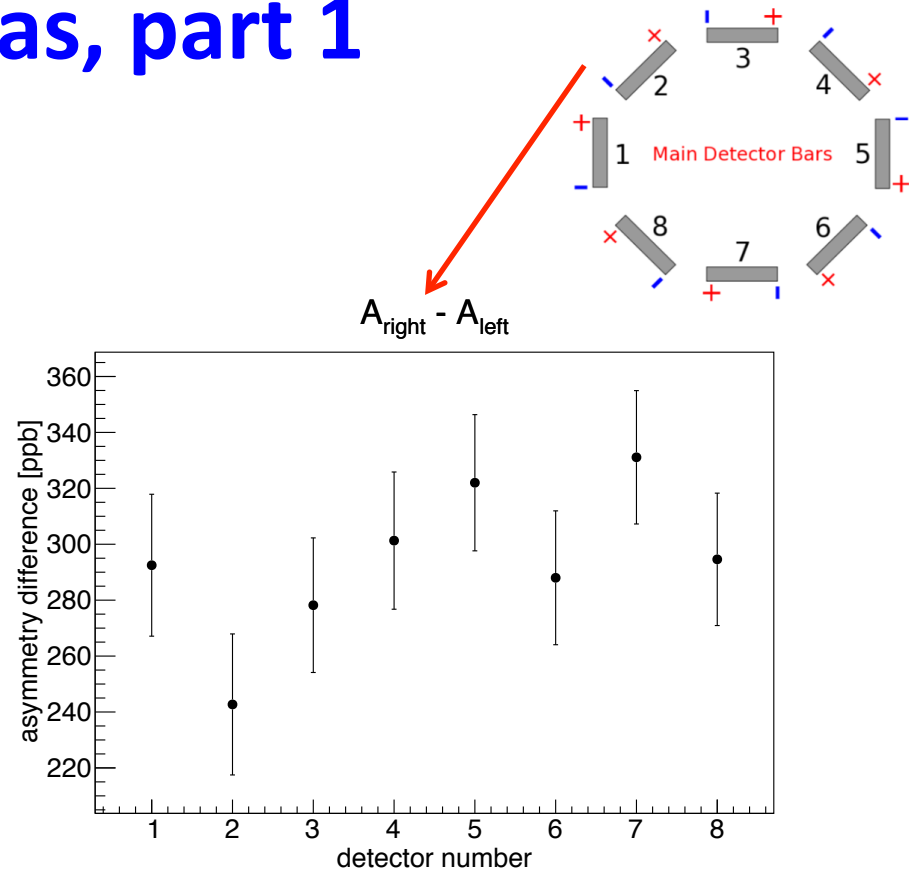
- The right and left PMT's saw different asymmetries. (by ~ 300 ppb) Why?
- Spin precession of scattered electron in QTOR magnet; some transverse polarization P_T
- P_T analyzed by scattering in Pb pre-radiators \rightarrow transverse asymmetry in detectors: opposite sign in the two PMTs (R & L) in each detector

$$A_{\text{diff}} = A_R - A_L \quad \text{Parity signal} = (A_R + A_L)/2 \quad \text{so effect cancels to first order.}$$

Need to determine the small residual non-cancellation (due to apparatus imperfections)

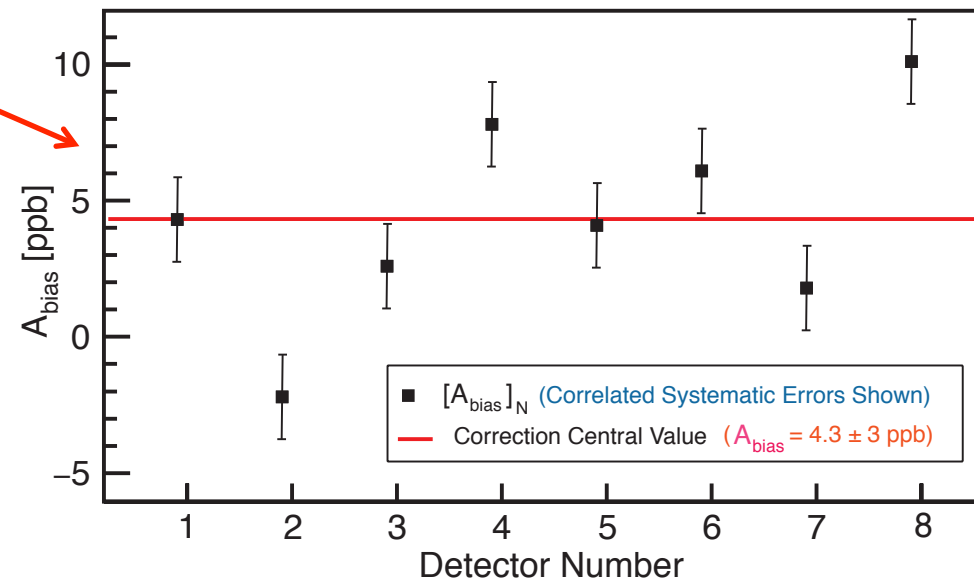
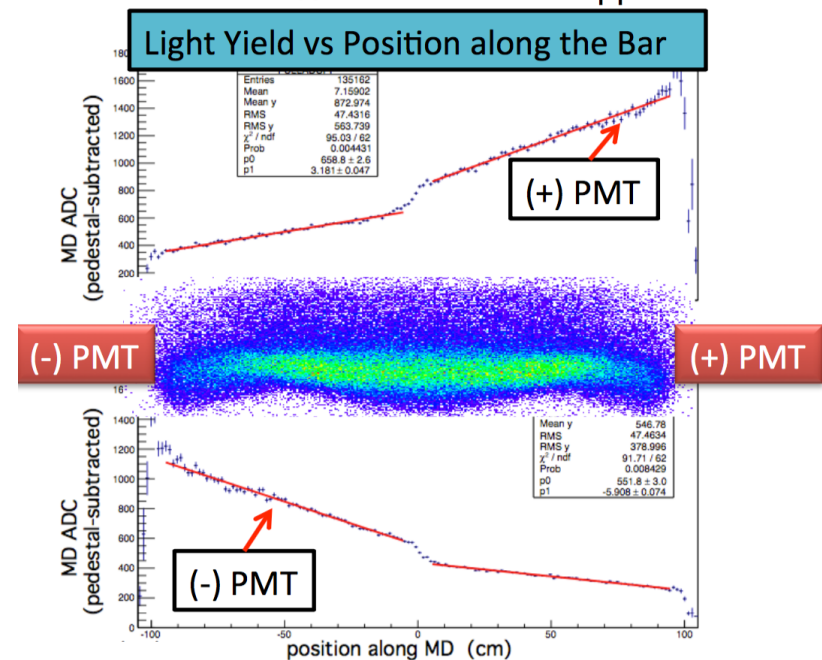
- Analyzing power in Pb:
 - Beam-normal single spin asymmetry (high energy): 2γ exchange
 - Mott scattering (low energy in EM shower)

(simulation shows that Mott scattering is the dominant contribution to A_{diff})



Rescattering Bias, Part 2

- For perfect symmetry, this effect cancels; minor broken symmetries of as-built apparatus lead to a **rescattering bias correction A_{bias}**
- Parity-conserving asymmetry in the rescattering process was studied in GEANT4; analytic effective models matching key features developed
- These were combined with
 - Scattered electron flux distributions
 - Tailored parameterizations of Cerenkov-light yield distributions for each bar (GEANT 4 optical photon transport with optical parameters tuned to match as-built bars)
- A_{bias} estimated for each individual bar
- Largest systematic uncertainty associated with optical modeling of as-built detectors (ie. uncertainty dominated by optical/mechanical imperfections - not details of Pb analyzing power)



Contributions to A_{bias} Uncertainty

Optical Model: ± 2.7 ppb

Simulation cross checks: ± 2.3 ppb

Glue Joints Effects: ± 1.5 ppb

Effective Model: ± 1.5 ppb

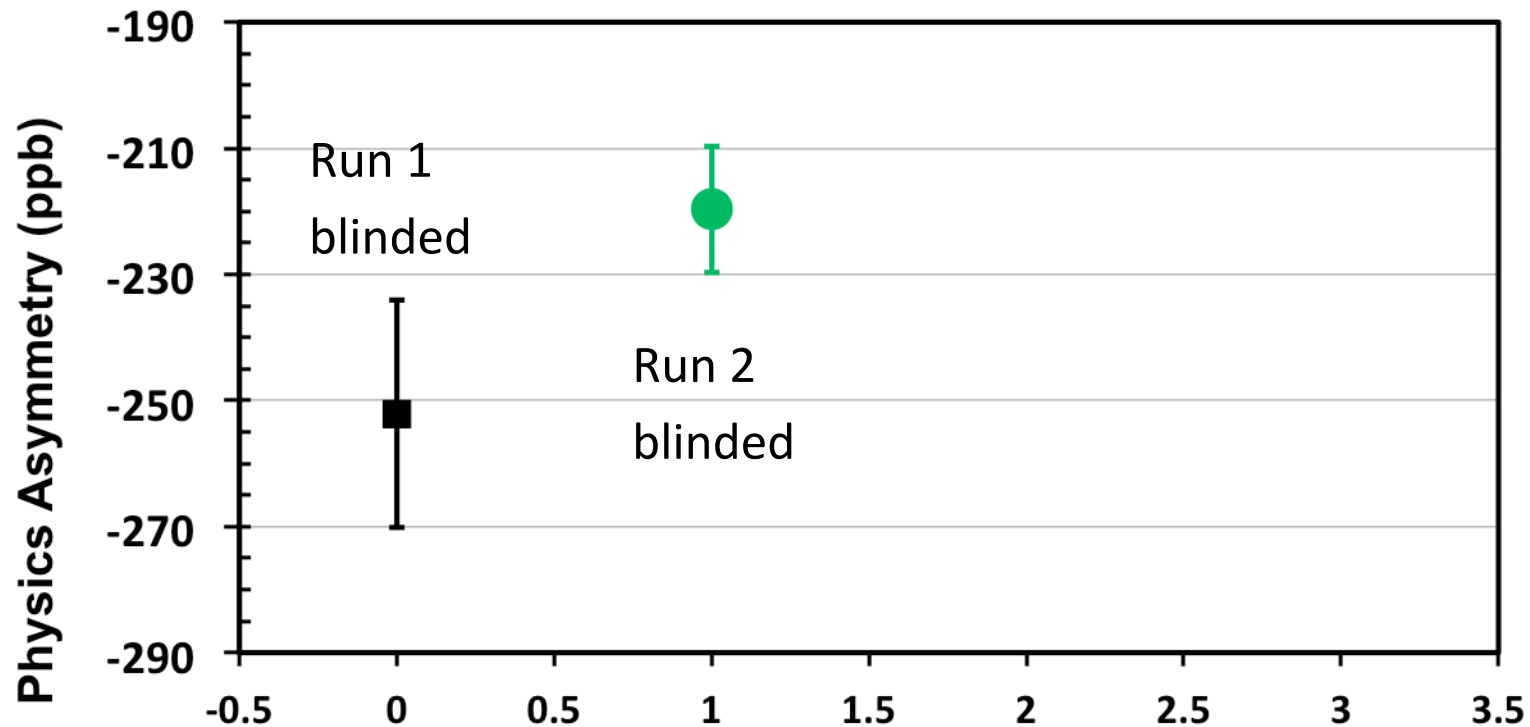
A_{bias} Correction: 4.3 ± 3.0 ppb

Unexpected, but high degree of symmetry made effect small.

Unblinding Day! March 31, 2017

Run 1 and 2 each had its own “blinding factor” (additive offset in range ± 60 ppb) to avoid analysis bias.

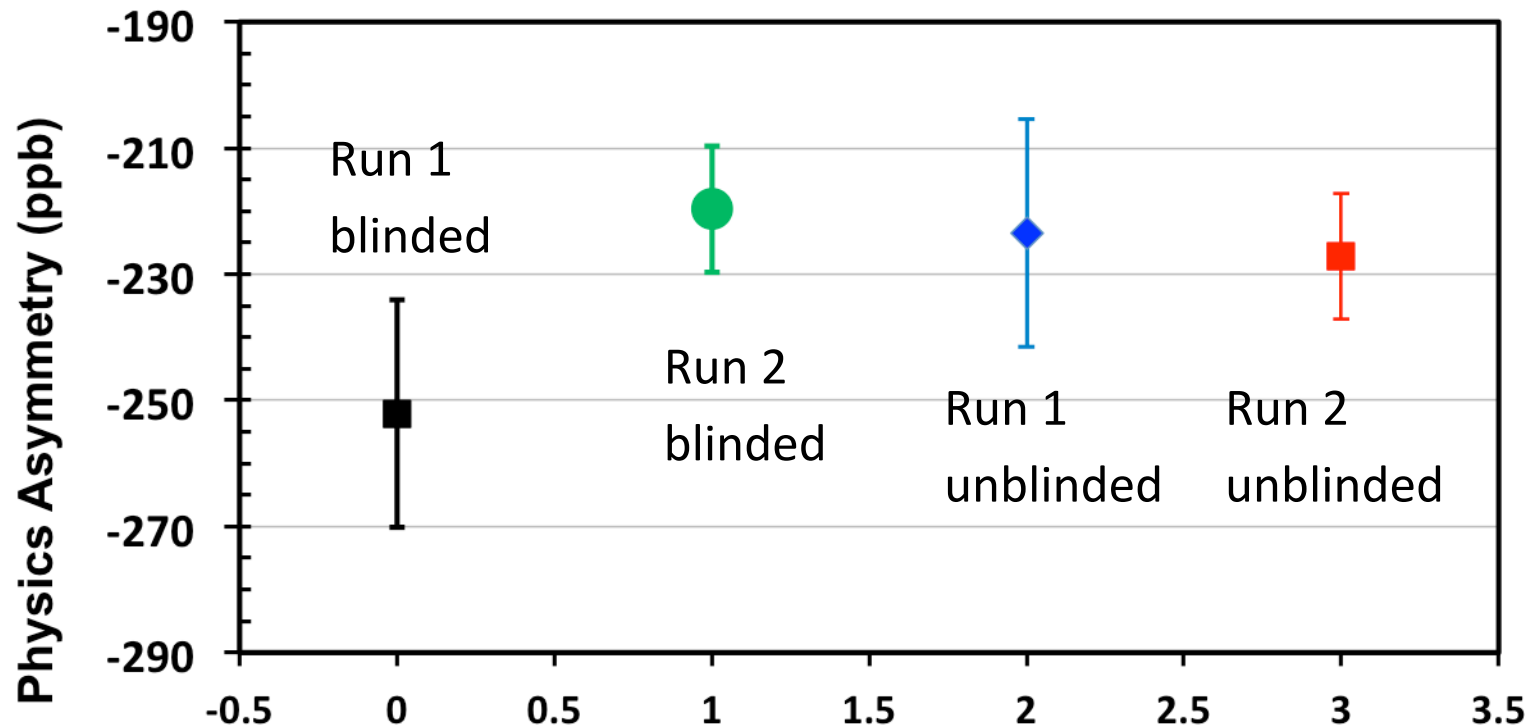
On March 31, 2017, after fully completing the analysis, we unblinded.



Unblinding Day! March 31, 2017

Run 1 and 2 each had its own “blinding factor” (additive offset in range ± 60 ppb) to avoid analysis bias.

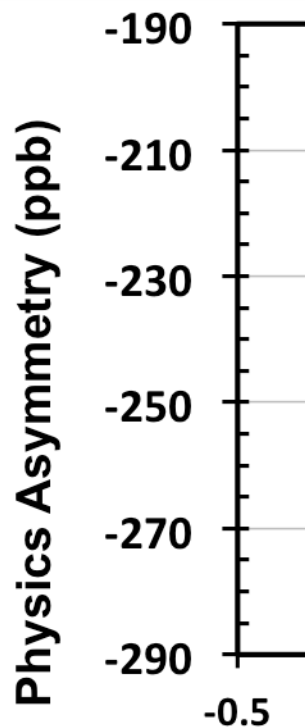
On March 31, 2017, after fully completing the analysis, we unblinded.



Unblinding Day! March 31, 2017

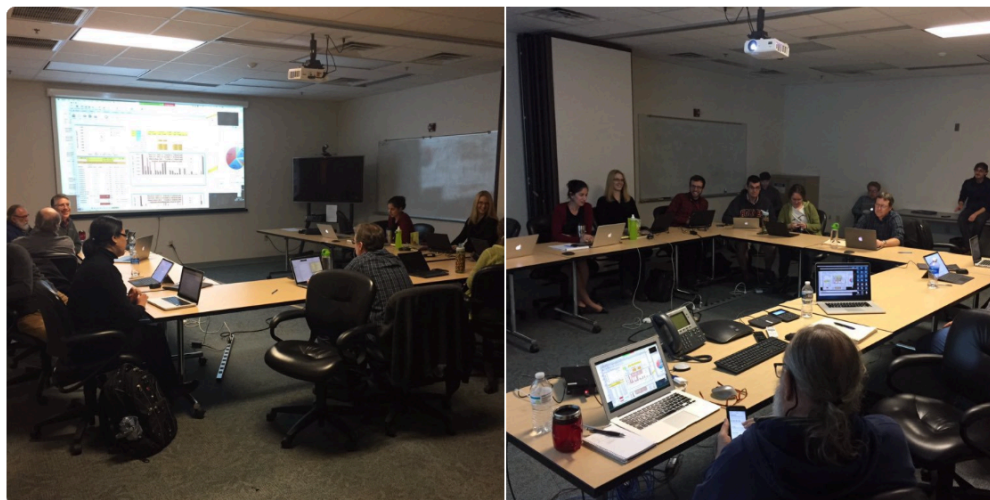
Run 1 and 2 each ha
ppb) to avoid analys
On March 31, 2017,

range ± 60
ended.



Mark L. Pitt
@marklpitt

Unblinding day for Qweak is here! Finally after 17 years!



4:38 PM - 31 Mar 2017

2 Retweets 8 Likes



Reply icon Retweet icon 2 Like icon 8 More options icon

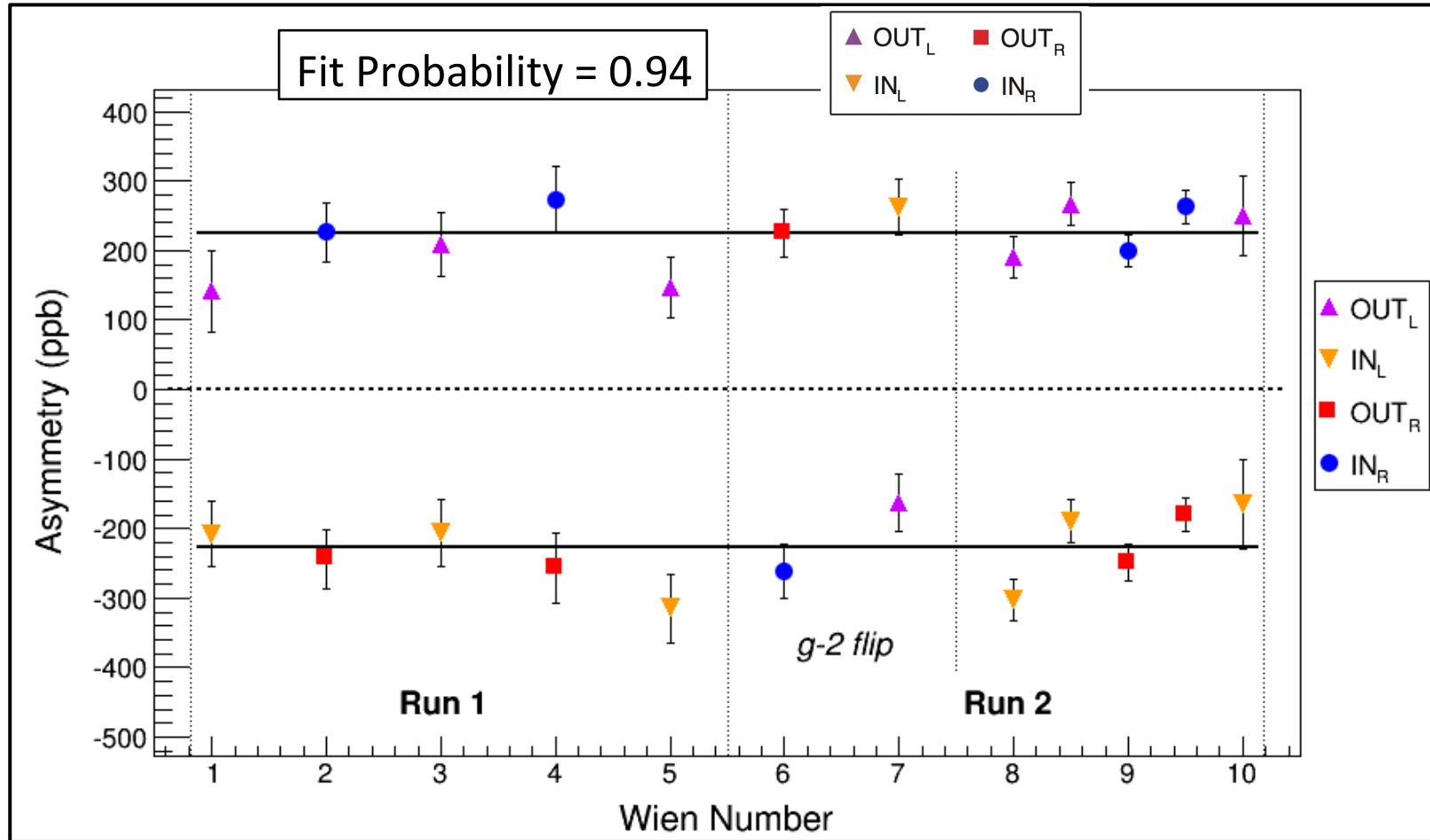


Tweet your reply

It didn't happen if you don't tweet about it!

Jefferson Lab Physics Seminar

Behavior of A_{ep} Under Slow Reversals



- Labels “IN or OUT” refer to status of IHWP.
- Subscript denotes setting of Wien filter as “Left” or “Right” correspond to 180 degree rotation of longitudinally polarized beam at target.

The data behaved as expected under all three types of slow helicity reversal.

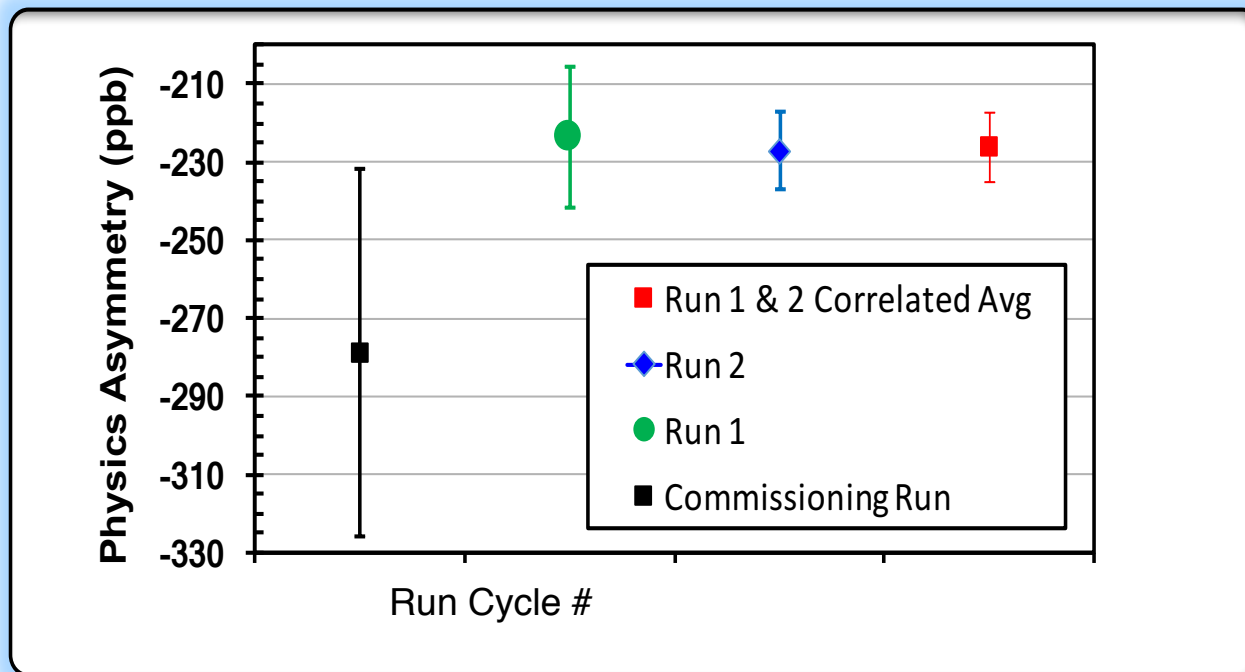
Combining the data without sign corrections gives:

$$\text{NULL average} = -1.75 \pm 6.51 \text{ ppb}$$

- consistent with zero as expected

Final $Q_{\text{weak}} A_{\text{ep}}$ Result

Period	Asymmetry (ppb)	Stat. Unc. (ppb)	Syst. Unc. (ppb)	Tot. Uncertainty (ppb)
Run 1	-223.5	15.0	10.1	18.0
Run 2	-227.2	8.3	5.6	10.0
Run 1 and 2 combined with correlations	-226.5	7.3	5.8	9.3



- Run 1 and 2 had different conditions and changes between runs that caused observable change in some of the beam-related systematic corrections
- The good agreement between the fully corrected asymmetries gives confidence in the result.

Extraction of Q_{weak} From e-p Asymmetry

$$A_{ep} = -226.5 \pm 7.3(\text{stat}) \pm 5.8(\text{syst}) \text{ ppb at } \langle Q^2 \rangle = 0.0249 \text{ (GeV/c)}^2$$

Global fit of world PVES data up to $Q^2 = 0.63 \text{ GeV}^2$ is done to extract the proton's weak charge

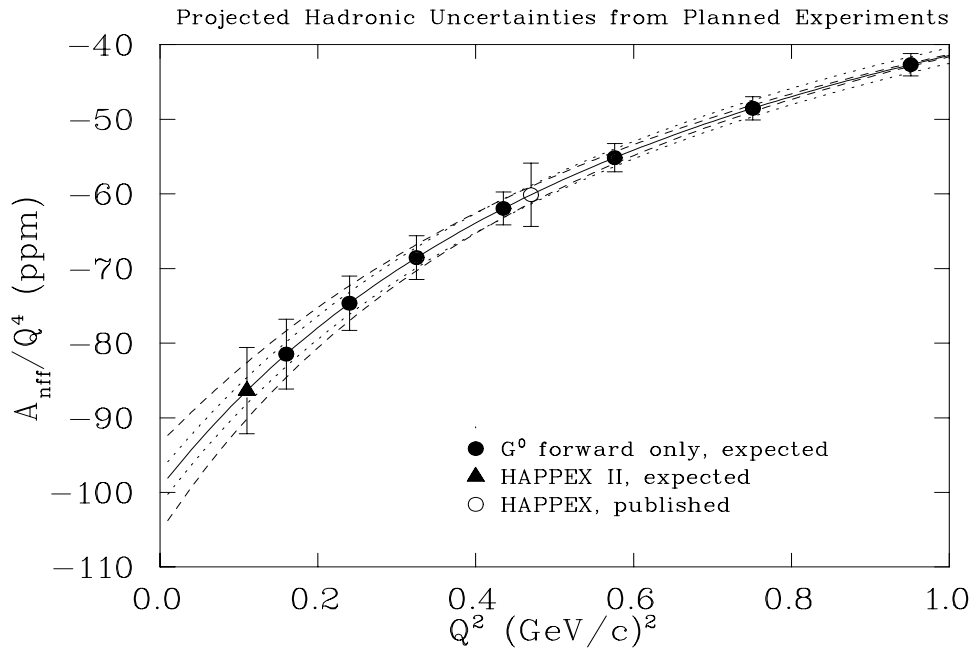
$$A_{ep}/A_0 = Q_W^p + Q^2 B(Q^2, \theta), \quad A_0 = \left[\frac{-G_F Q^2}{4\pi\alpha\sqrt{2}} \right].$$

Extraction of Q_{weak} From e-p Asymmetry

$$A_{ep} = -226.5 \pm 7.3(\text{stat}) \pm 5.8(\text{syst}) \text{ ppb at } \langle Q^2 \rangle = 0.0249 \text{ (GeV/c)}^2$$

Global fit of world PVES data up to $Q^2 = 0.63 \text{ GeV}^2$ is done to extract the proton's weak charge

$$A_{ep}/A_0 = Q_W^p + Q^2 B(Q^2, \theta), \quad A_0 = \left[\frac{-G_F Q^2}{4\pi\alpha\sqrt{2}} \right].$$



At time of proposal in 2001, lots of planned PVES experiments, but only 2 published ones on e-p.

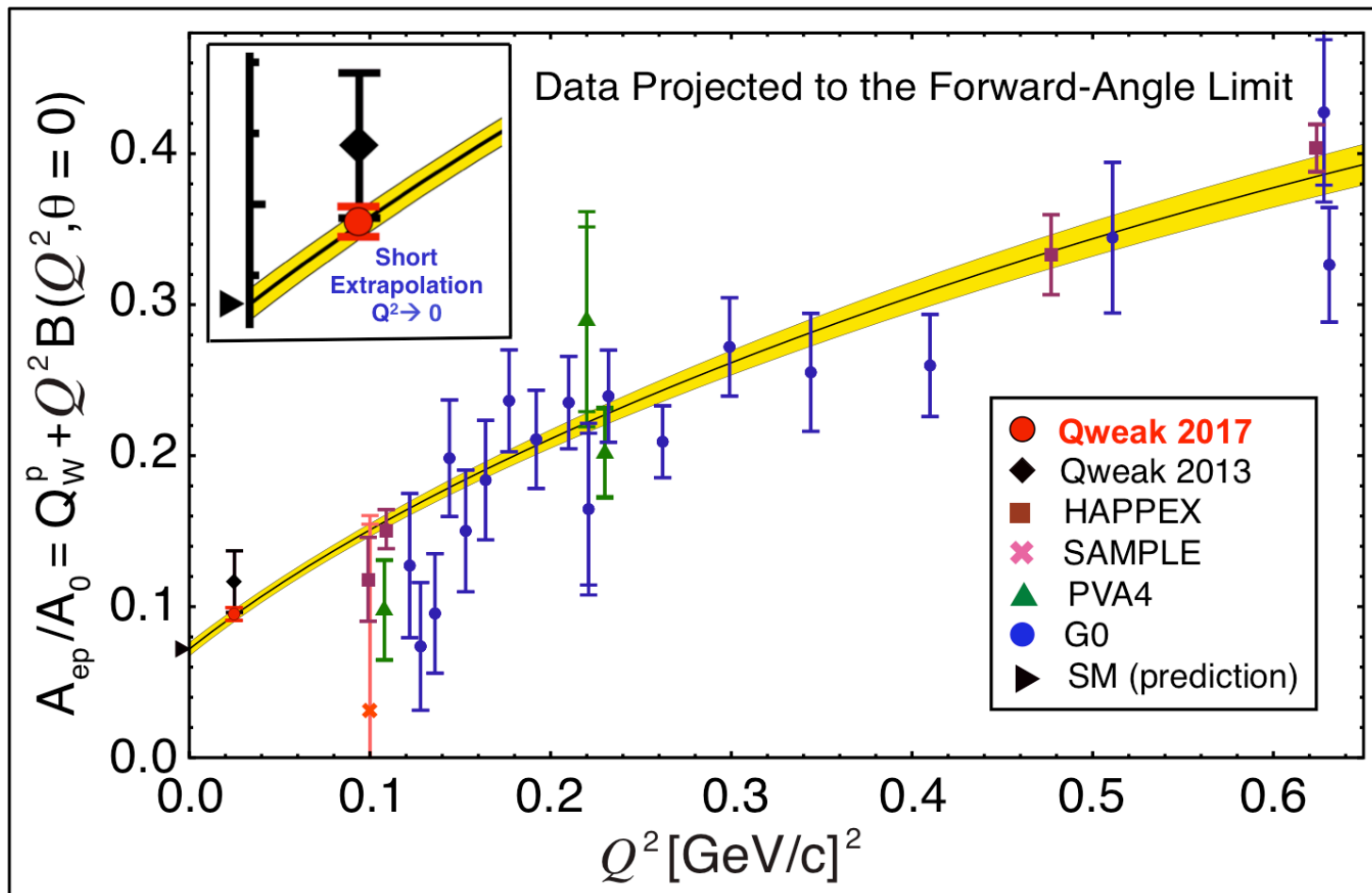
Extraction of Q_{weak} From e-p Asymmetry

$$A_{ep} = -226.5 \pm 7.3(\text{stat}) \pm 5.8(\text{syst}) \text{ ppb at } \langle Q^2 \rangle = 0.0249 \text{ (GeV/c)}^2$$

Global fit of world PVES data up to $Q^2 = 0.63 \text{ GeV}^2$ is done to extract the proton's weak charge

$$A_{ep}/A_0 = Q_W^p + Q^2 B(Q^2, \theta), \quad A_0 = \left[\frac{-G_F Q^2}{4\pi\alpha\sqrt{2}} \right].$$

Today: 33 entries in PVES (e-p, e-d, e-⁴He) database



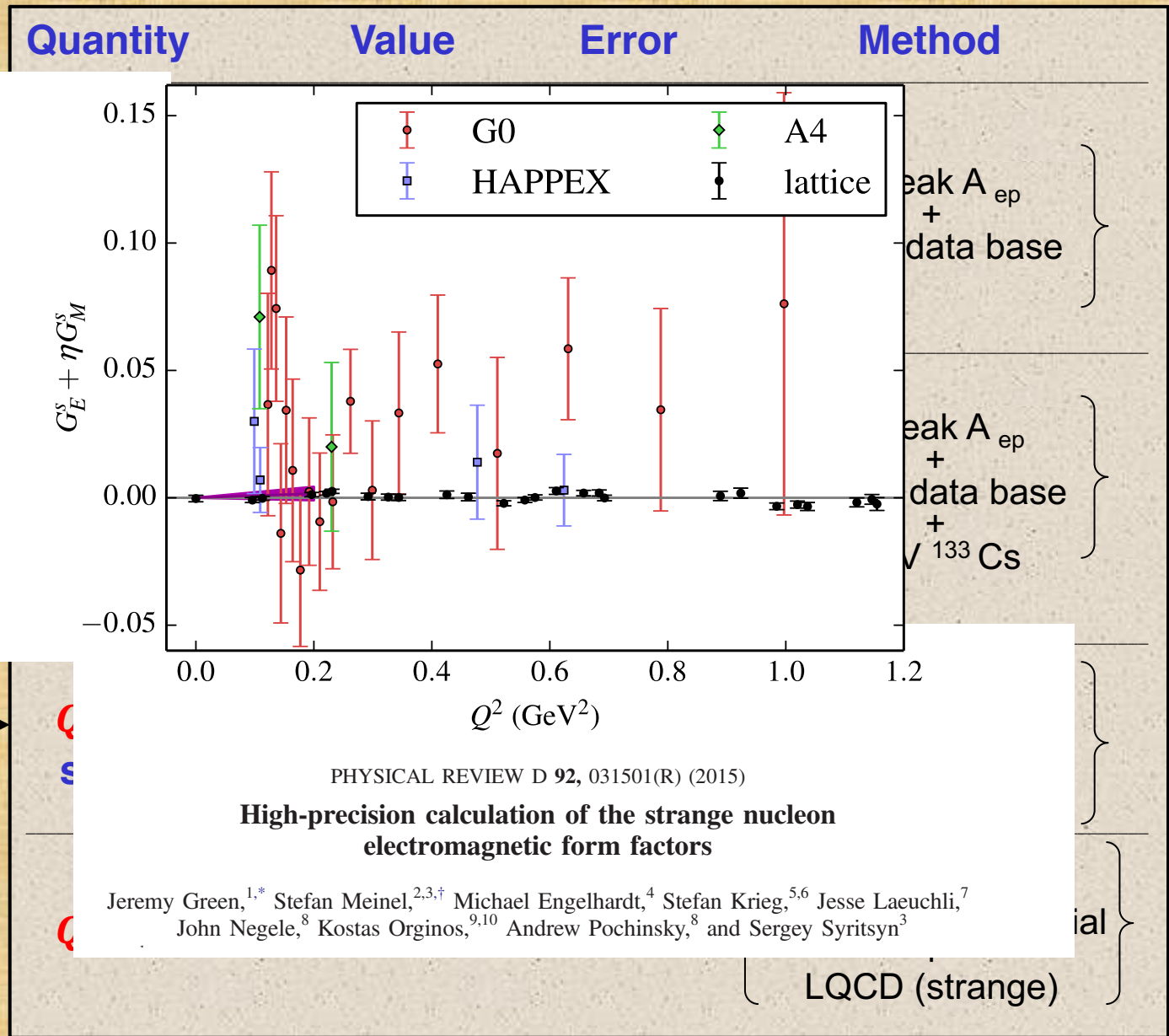
Summary of Results from Q_{weak}

**Addition of
Lattice QCD
constraint on
strange
quarks further
improves
precision of
 Q_W^p & $\sin^2\theta_W$**

Quantity	Value	Error	Method
Q_W^p	0.0719	0.0045	$\left\{ \begin{array}{l} \text{Qweak } A_{ep} \\ + \\ \text{PVES data base} \end{array} \right\}$
$\sin^2\theta_W$	0.2382	0.0011	
ρ_s	0.19	0.11	
μ_s	-0.18	0.15	
$G_A^{Z(T=1)}$	-0.67	0.33	
Q_W^p	0.0718	0.0045	$\left\{ \begin{array}{l} \text{Qweak } A_{ep} \\ + \\ \text{PVES data base} \\ + \\ \text{APV } ^{133}\text{Cs} \end{array} \right\}$
Q_W^n	-0.9808	0.0063	
C_{1u}	-0.1874	0.0022	
C_{1d}	0.3389	0.0025	
C_1 correlation =	-0.9317		
Q_W^p	0.0684	0.0039	$\left\{ \begin{array}{l} \text{Qweak } A_{ep} \\ + \\ \text{PVES data base} \\ + \\ \text{LQCD (strange)} \end{array} \right\}$
$\sin^2\theta_W$	0.2392	0.0009	
Q_W^p	0.0706	0.0047	$\left\{ \begin{array}{l} \text{Qweak } A_{ep} \\ + \\ \text{EMFF's \& theory axial} \\ + \\ \text{LQCD (strange)} \end{array} \right\}$

Summary of Results from Q_{weak}

**Addition of
Lattice QCD
constraint on
strange
quarks further
improves
precision of
 Q_W^p & $\sin^2\theta_W$**



Summary of Results from Q_{weak}

Including
 ^{133}Cs APV result
 allows
 extraction of
 neutron weak
 charge
 &
 separation of
 C_{1u} , C_{1d} quark
 coupling
 constants

Quantity	Value	Error	Method
Q_W^p	0.0719	0.0045	$\left\{ \begin{array}{c} \text{Qweak } A_{ep} \\ + \\ \text{PVES data base} \end{array} \right\}$
$\sin^2\theta_W$	0.2382	0.0011	
ρ_s	0.19	0.11	
μ_s	-0.18	0.15	
$G_A^{Z(T=1)}$	-0.67	0.33	
Q_W^p	0.0718	0.0045	$\left\{ \begin{array}{c} \text{Qweak } A_{ep} \\ + \\ \text{PVES data base} \\ + \\ \text{APV } ^{133}\text{Cs} \end{array} \right\}$
Q_W^n	-0.9808	0.0063	
C_{1u}	-0.1874	0.0022	
C_{1d}	0.3389	0.0025	
C_1 correlation =	-0.9317		
Q_W^p	0.0684	0.0039	$\left\{ \begin{array}{c} \text{Qweak } A_{ep} \\ + \\ \text{PVES data base} \\ + \\ \text{LQCD (strange)} \end{array} \right\}$
$\sin^2\theta_W$	0.2392	0.0009	
Q_W^p	0.0706	0.0047	$\left\{ \begin{array}{c} \text{Qweak } A_{ep} \\ + \\ \text{EMFF's \& theory axial} \\ + \\ \text{LQCD (strange)} \end{array} \right\}$

Summary of Results from Q_{weak}

Precision of A_{ep}
dominates
determination
of Q_W^p

Alternate
“Standalone”
technique to
extract Q_W^p
does **NOT**
depend on
other PV
measurements

Quantity	Value	Error	Method
Q_W^p	0.0719	0.0045	$\left\{ \begin{array}{c} \text{Qweak } A_{ep} \\ + \\ \text{PVES data base} \end{array} \right\}$
$\sin^2\theta_W$	0.2382	0.0011	
ρ_s	0.19	0.11	
μ_s	-0.18	0.15	
$G_A^{Z(T=1)}$	-0.67	0.33	
Q_W^p	0.0718	0.0045	$\left\{ \begin{array}{c} \text{Qweak } A_{ep} \\ + \\ \text{PVES data base} \\ + \\ \text{APV } ^{133}\text{Cs} \end{array} \right\}$
Q_W^n	-0.9808	0.0063	
C_{1u}	-0.1874	0.0022	
C_{1d}	0.3389	0.0025	
C_1 correlation =	-0.9317		
Q_W^p	0.0684	0.0039	$\left\{ \begin{array}{c} \text{Qweak } A_{ep} \\ + \\ \text{PVES data base} \\ + \\ \text{LQCD (strange)} \end{array} \right\}$
$\sin^2\theta_W$	0.2392	0.0009	
Q_W^p	0.0706	0.0047	$\left\{ \begin{array}{c} \text{Qweak } A_{ep} \\ + \\ \text{EMFF's \& theory axial} \\ + \\ \text{LQCD (strange)} \end{array} \right\}$

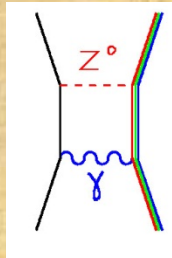
Electroweak Radiative Corrections

Q_W^p Standard Model ($Q^2 = 0$) [2016]	0.0708 ± 0.0003
Q_W^p Experiment Final Uncertainty [2017]	± 0.0045

$$Q_W^p = [1 + \Delta\rho + \Delta_e] [(1 - 4 \sin^2 \theta_W(0)) + \Delta_{e'}] + \square_{WW} + \square_{ZZ} + \square_{\gamma Z}$$

Correction to Q_W^p	Uncertainty
$\Delta \sin \theta_W (M_Z)$	± 0.0006
$Z\gamma$ box (6.4% \pm 0.6%)	0.00459 ± 0.00044
$\Delta \sin \theta_W (Q)_{hadronic}$	± 0.0003
WW, ZZ box - pQCD	± 0.0001
Charge symmetry	0
Total	± 0.0008

Erlar et al., PRD 68(2003)016006.



Calculations of Two Boson Exchange effects on Q_W^p at our Kinematics:

Recent theory calculations applied to entire data set of PV measurements as appropriate in global analysis.

Our ΔA_{ep} precise enough that corrections to higher Q^2 points make little difference in extrapolation to zero Q^2 .

Energy Dependence γZ correction:

Hall, N.L., Blunden, P.G., Melnitchouk, W., Thomas, A.W., Young, R.D. Quark-hadron duality constraints on γZ box corrections to parity-violating elastic scattering. *Phys. Lett. B* 753, 221-226 (2016).

Axial Vector γZ correction:

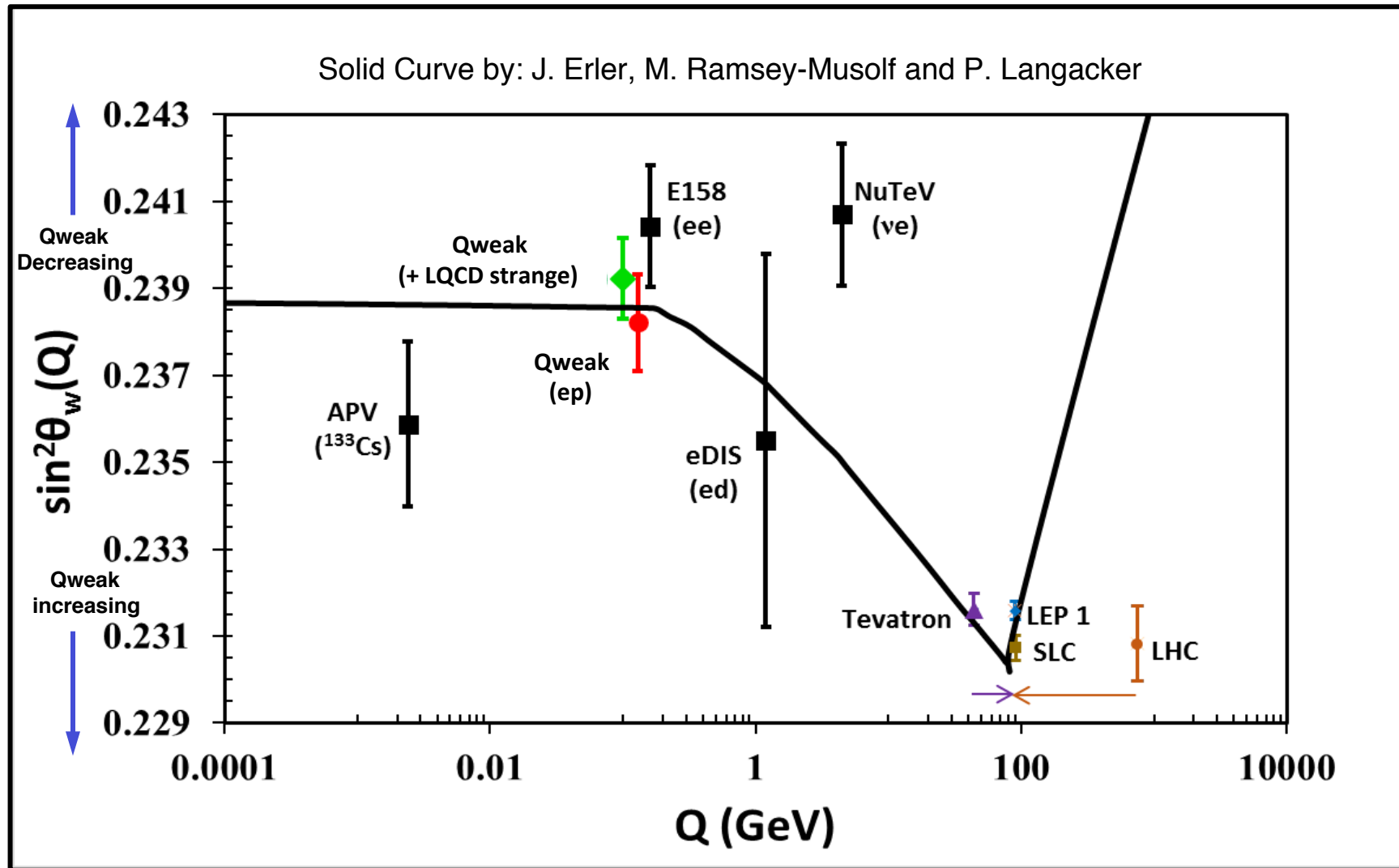
Peter Blunden, P.G., Melnitchouk, W., Thomas, A.W. New Formulation of γZ Box Corrections to the Weak Charge of the Proton. *Phys. Rev. Lett.* 107, 081801 (2011).

Q^2 Dependence γZ :

Gorchtein, M., Horowitz, C.J., Ramsey-Musolf, M.J. Model dependence of the γZ dispersion correction to the parity-violating asymmetry in elastic ep scattering. *Phys. Rev. C* 84, 015502 (2011).

Running of the Weak Mixing Angle $\sin^2\theta_w$

Q_{weak} completes the low Q^2 “weak charge triad” by adding a precision measurement of the proton’s weak charge.



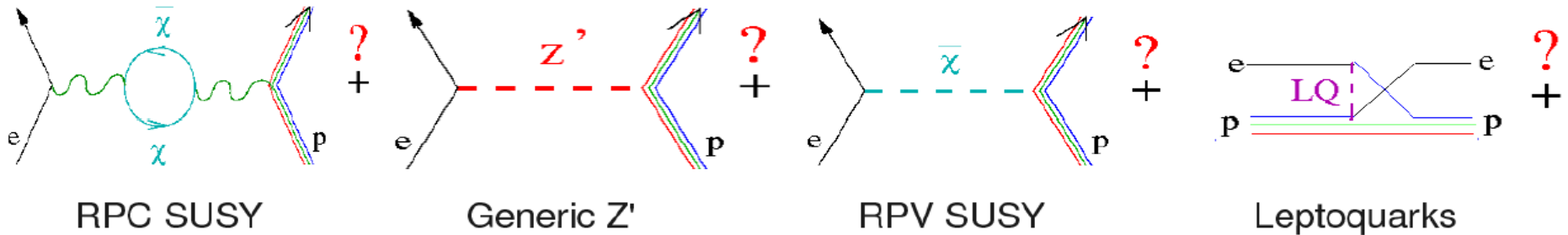
Note: interference effects of heavy new physics (ie. Z' , leptoquarks) is suppressed at Z resonance so LEP/SLC mass limits $\sim < \text{TeV}$, while low energy observables probe few TeV scale

Outline

- Motivation and formalism
- Experiment: technical challenges and achievements
- Analysis: Key systematic uncertainties and extraction of the proton's weak charge
- Implications of the new precision measurement of the proton's weak charge

Sensitivity to New Physics at TeV Scales

Possible New Physics at multi-TeV scales:



Parameterize these scenarios in a general way with a new contact interaction in the Lagrangian:

$$\mathcal{L}_{\text{NC}}^{\text{eq}} = -\frac{G_F}{\sqrt{2}} \bar{e} \gamma_\mu \gamma_5 e \sum_q C_{1q} \bar{q} \gamma^\mu q.$$

$$\mathcal{L}_{\text{NP}}^{\text{PV}} = -\frac{g^2}{\Lambda^2} \bar{e} \gamma_\mu \gamma_5 e \sum_q h_V^q \bar{q} \gamma^\mu q \quad \begin{array}{l} g=\text{coupling} \\ \Lambda=\text{mass scale} \end{array}$$

Arbitrary quark flavor dependence of new physics:

$$h_V^u = \cos \theta_h \quad h_V^d = \sin \theta_h$$

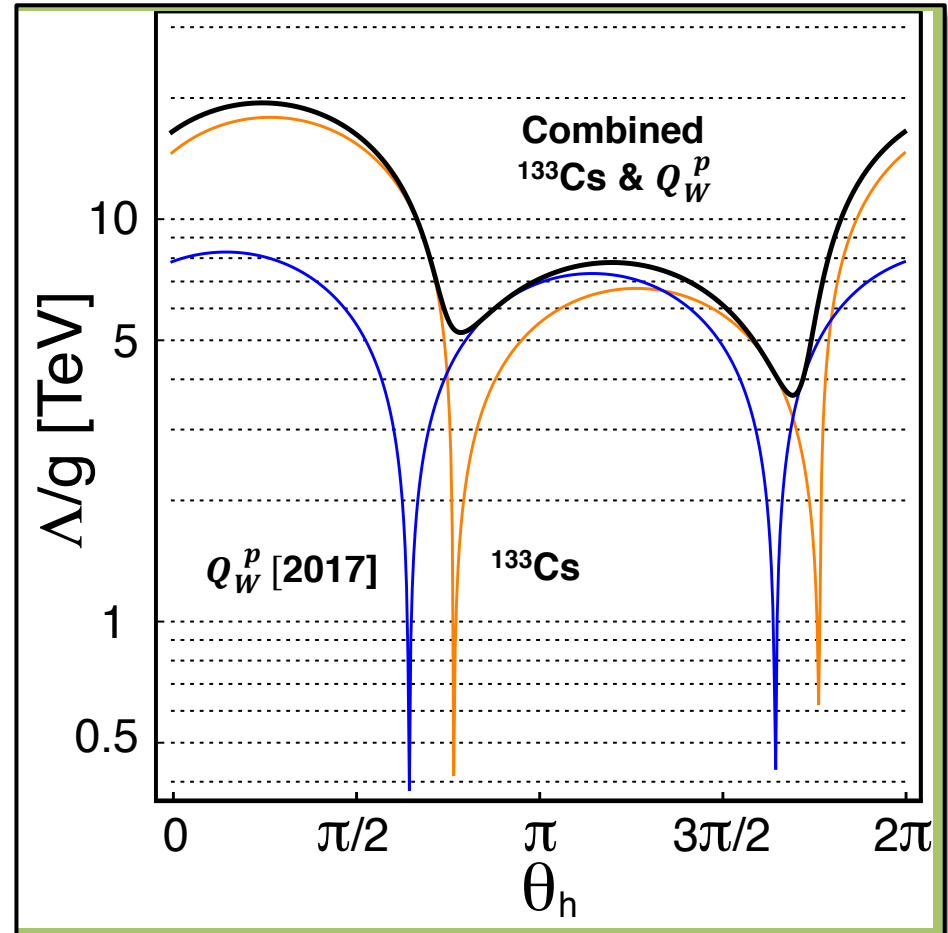
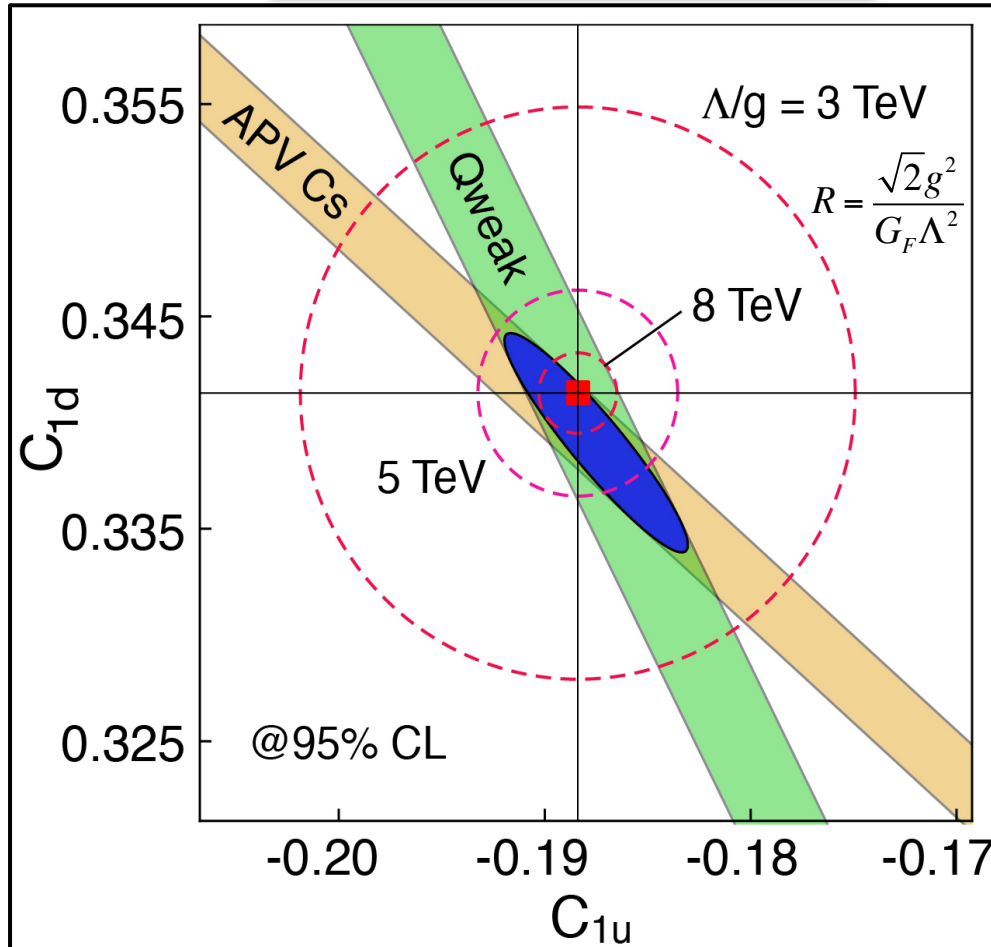
Limits on Semi-Leptonic PV Physics Beyond SM

$$\mathcal{L}_{\text{NP}}^{\text{PV}} = -\frac{g^2}{\Lambda^2} \bar{e} \gamma_\mu \gamma_5 e \sum_q h_V^q \bar{q} \gamma^\mu q$$

$$h_V^u = \cos \theta_h \quad h_V^d = \sin \theta_h$$

$$Q_W^p = -2(2C_{1u} + C_{1d})$$

**New Physics Ruled Out
@95% CL Below Mass Scale of Λ/g**



SM is red square. Dashed contours indicate value of $\Lambda/g = 3, 5, \text{ and } 8 \text{ TeV}$.
(^{133}Cs APV, from PDG – Flambaum)

θ_h is “flavor mixing angle” in Lagrangian $\mathcal{L}_{\text{NP}}^{\text{PV}}$ for new physics at value Λ/g mapped around boundary of experimental limits.

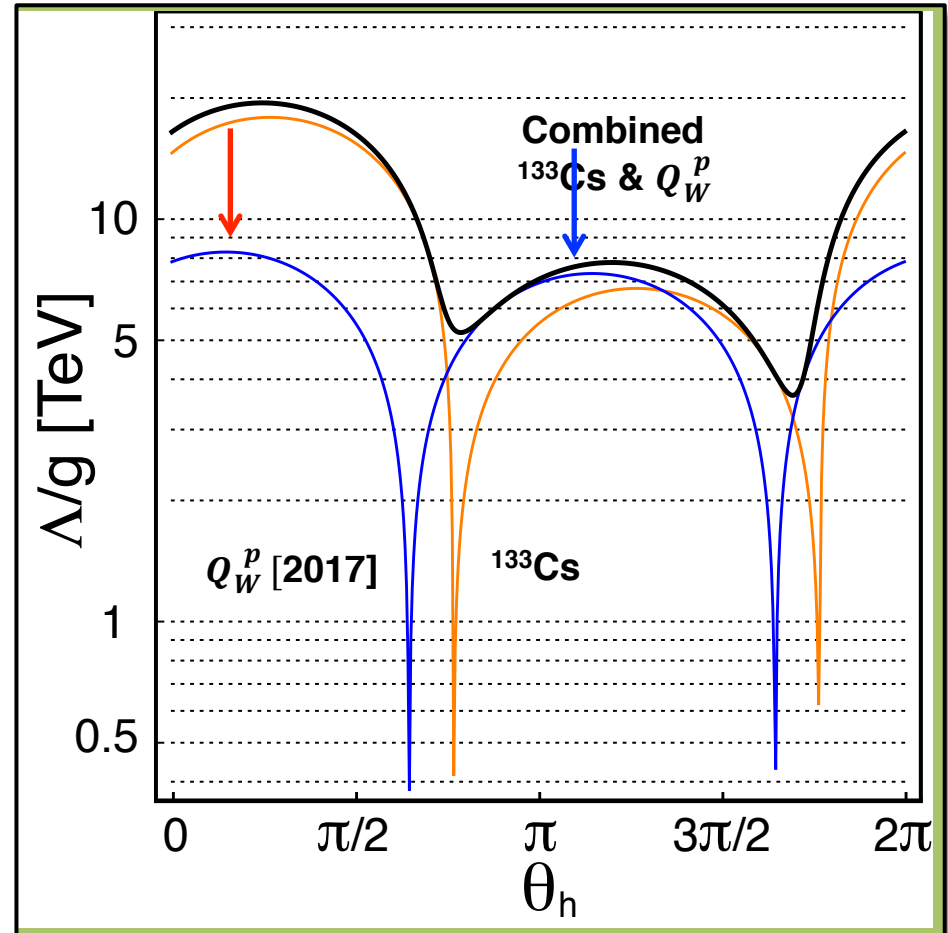
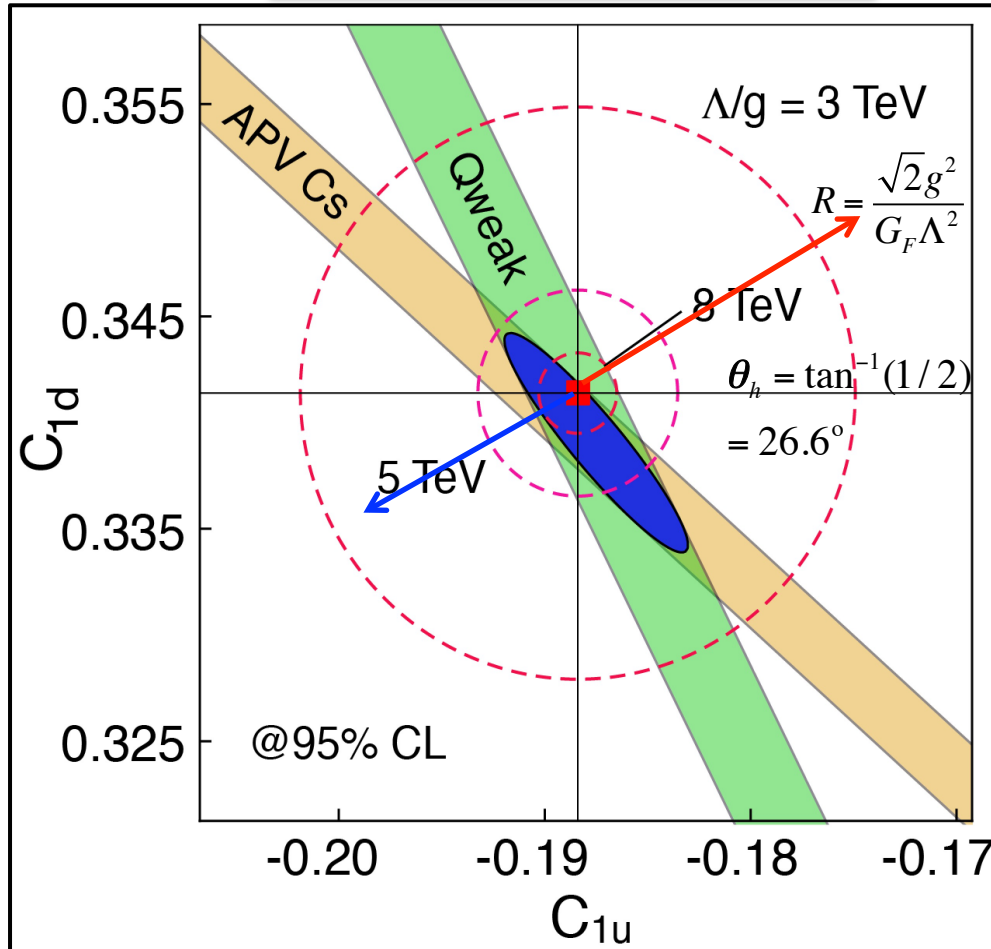
Limits on Semi-Leptonic PV Physics Beyond SM

$$\mathcal{L}_{\text{NP}}^{\text{PV}} = -\frac{g^2}{\Lambda^2} \bar{e} \gamma_\mu \gamma_5 e \sum_q h_V^q \bar{q} \gamma^\mu q$$

$$h_V^u = \cos \theta_h \quad h_V^d = \sin \theta_h$$

$$Q_W^p = -2(2C_{1u} + C_{1d})$$

**New Physics Ruled Out
@95% CL Below Mass Scale of Λ/g**



SM is red square. Dashed contours indicate value of $\Lambda/g = 3, 5, \text{ and } 8 \text{ TeV}$.
 (^{133}Cs APV, from PDG – Flambaum)

θ_h is “flavor mixing angle” in Lagrangian $\mathcal{L}_{\text{NP}}^{\text{PV}}$ for new physics at value Λ/g mapped around boundary of experimental limits.

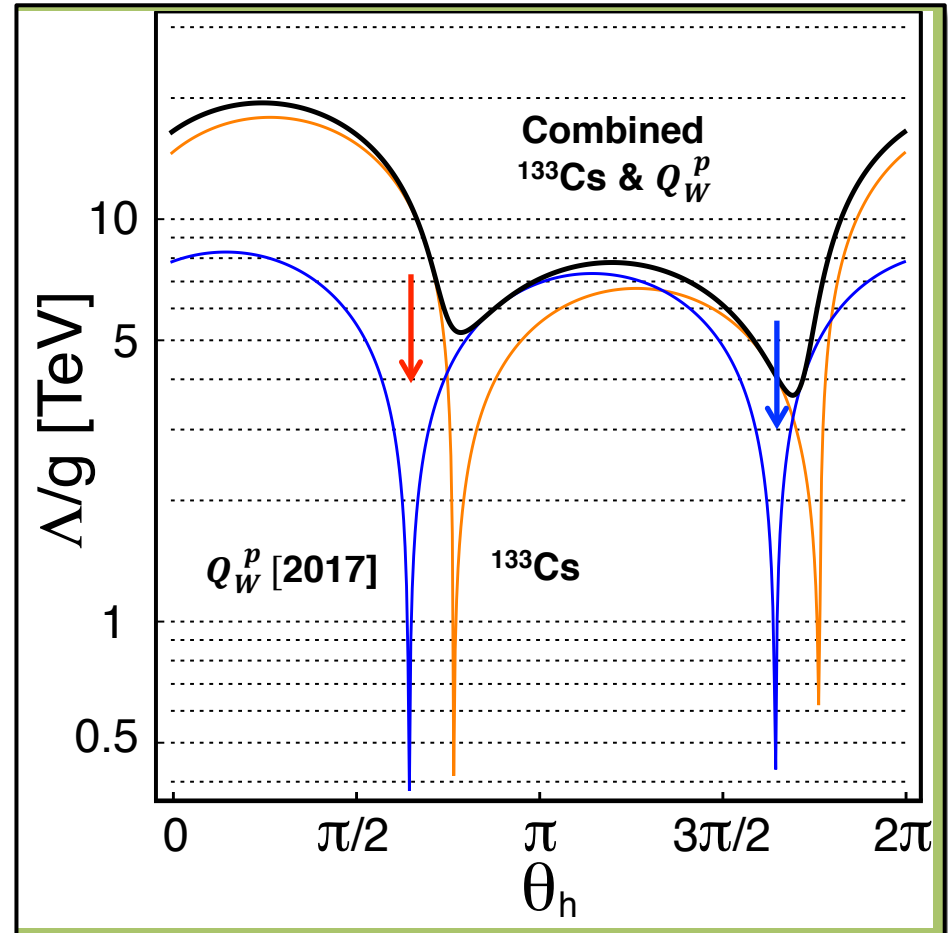
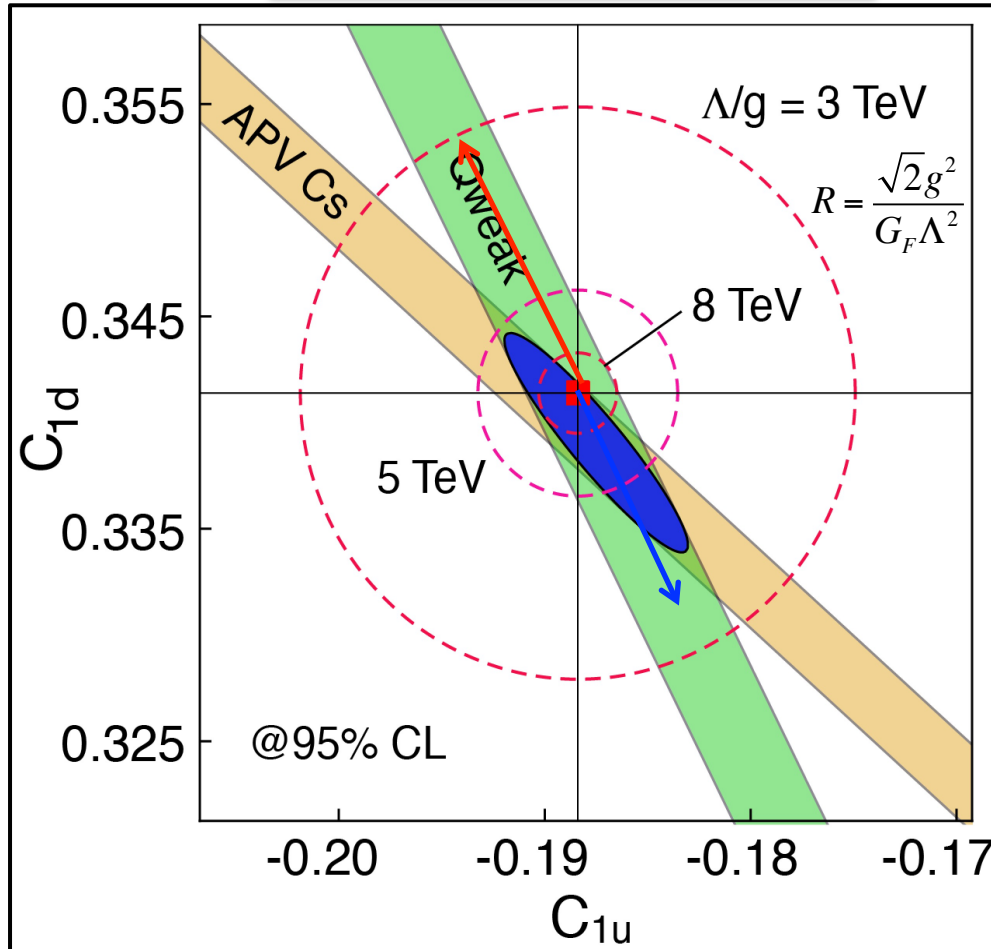
Limits on Semi-Leptonic PV Physics Beyond SM

$$\mathcal{L}_{\text{NP}}^{\text{PV}} = -\frac{g^2}{\Lambda^2} \bar{e} \gamma_\mu \gamma_5 e \sum_q h_V^q \bar{q} \gamma^\mu q$$

$$h_V^u = \cos \theta_h \quad h_V^d = \sin \theta_h$$

$$Q_W^p = -2(2C_{1u} + C_{1d})$$

**New Physics Ruled Out
@95% CL Below Mass Scale of Λ/g**



SM is red square. Dashed contours indicate value of $\Lambda/g = 3, 5, \text{ and } 8 \text{ TeV}$.
(^{133}Cs APV, from PDG – Flambaum)

θ_h is “flavor mixing angle” in Lagrangian $\mathcal{L}_{\text{NP}}^{\text{PV}}$ for new physics at value Λ/g mapped around boundary of experimental limits.

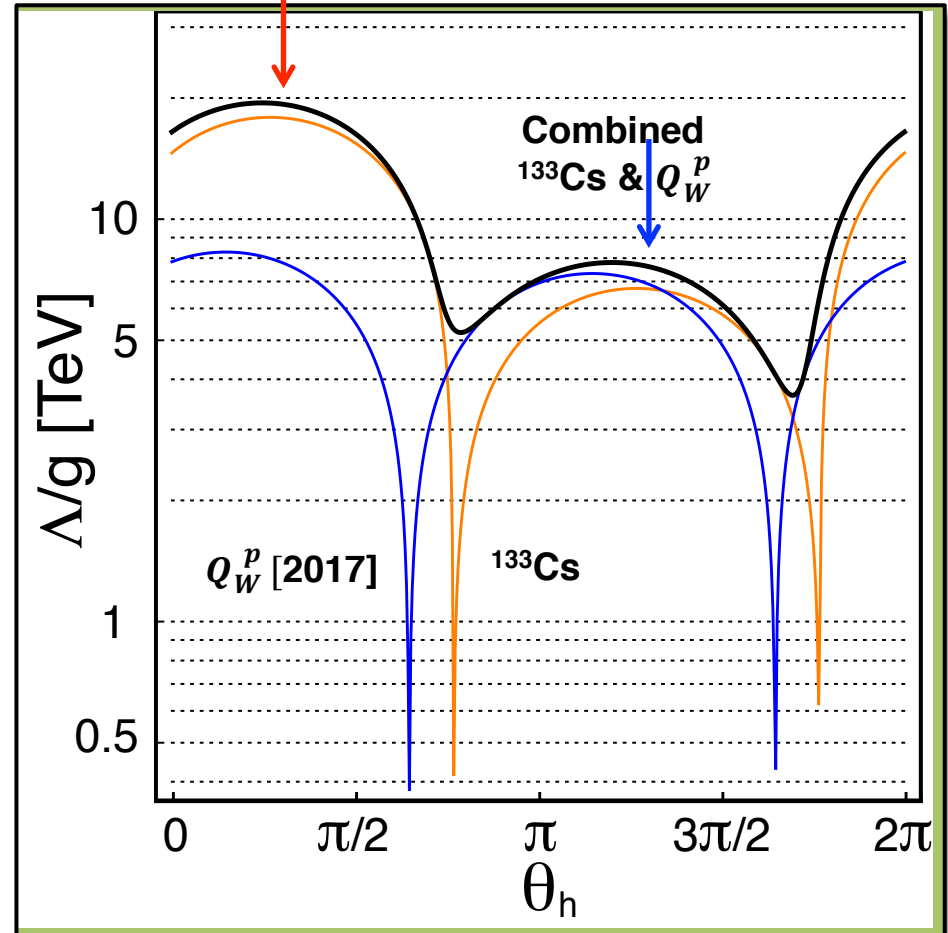
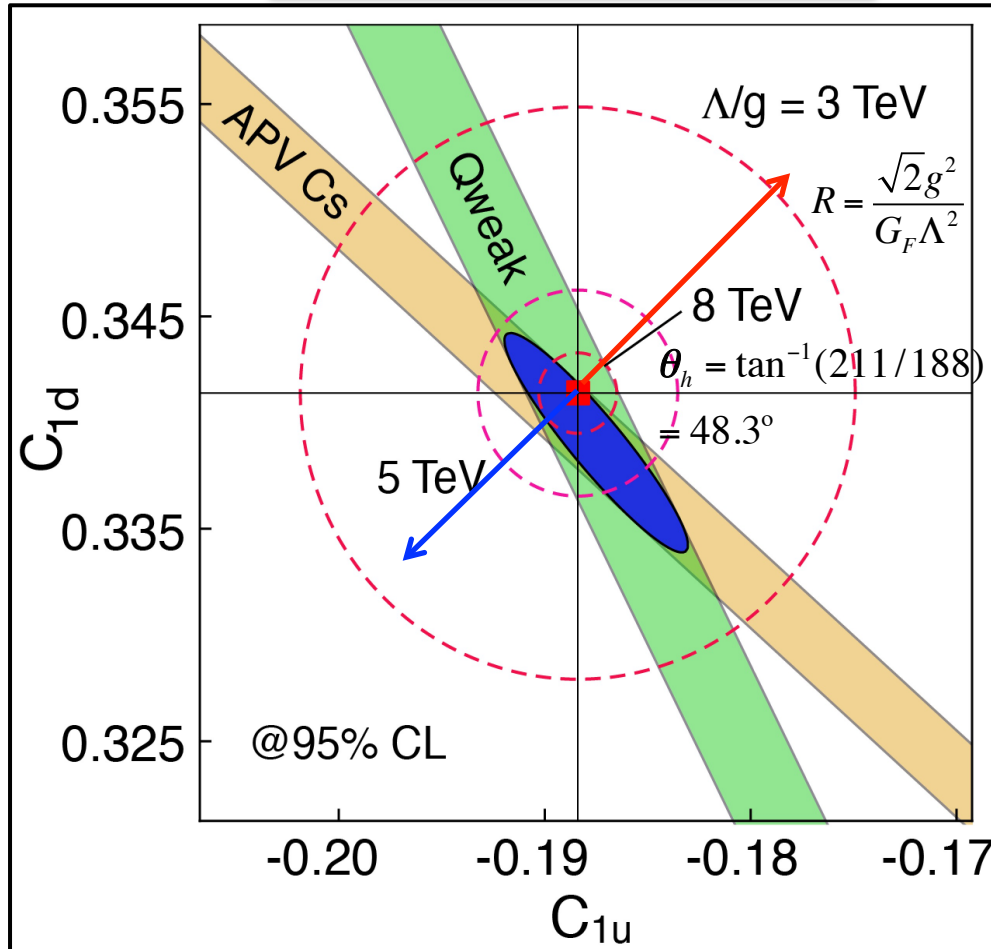
Limits on Semi-Leptonic PV Physics Beyond SM

$$\mathcal{L}_{\text{NP}}^{\text{PV}} = -\frac{g^2}{\Lambda^2} \bar{e} \gamma_\mu \gamma_5 e \sum_q h_V^q \bar{q} \gamma^\mu q$$

$$h_V^u = \cos \theta_h \quad h_V^d = \sin \theta_h$$

$$Q_W^p = -2(2C_{1u} + C_{1d})$$

**New Physics Ruled Out
@95% CL Below Mass Scale of Λ/g**



SM is red square. Dashed contours indicate value of $\Lambda/g = 3, 5, \text{ and } 8 \text{ TeV}$.
(^{133}Cs APV, from PDG – Flambaum)

θ_h is “flavor mixing angle” in Lagrangian $\mathcal{L}_{\text{NP}}^{\text{PV}}$ for new physics at value Λ/g mapped around boundary of experimental limits.

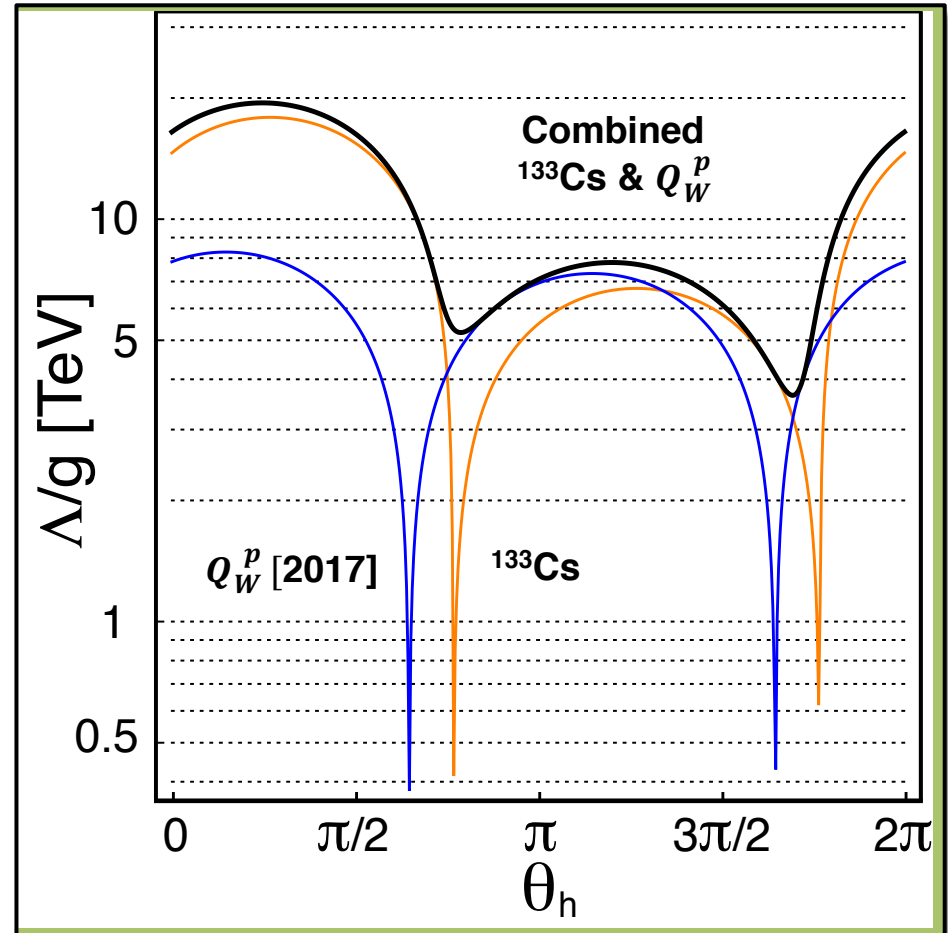
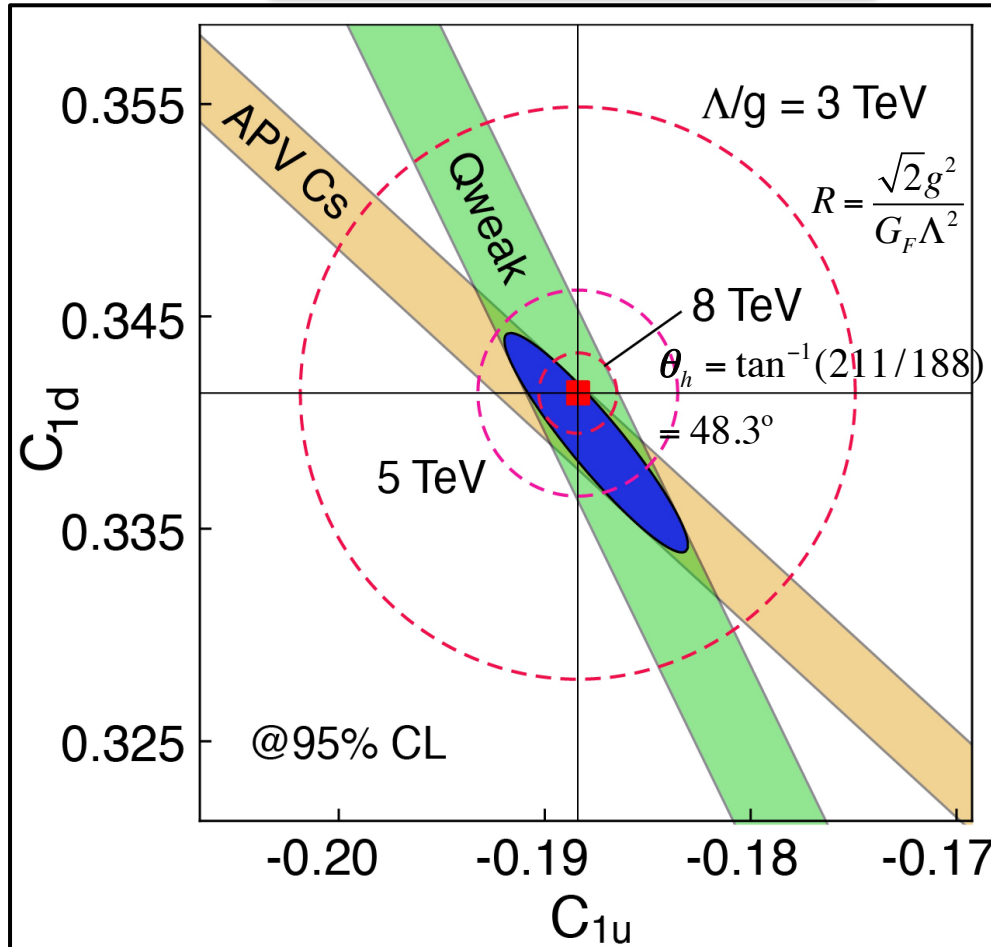
Limits on Semi-Leptonic PV Physics Beyond SM

$$\mathcal{L}_{\text{NP}}^{\text{PV}} = -\frac{g^2}{\Lambda^2} \bar{e} \gamma_\mu \gamma_5 e \sum_q h_V^q \bar{q} \gamma^\mu q$$

$$h_V^u = \cos \theta_h \quad h_V^d = \sin \theta_h$$

$$Q_W^p = -2(2C_{1u} + C_{1d})$$

**New Physics Ruled Out
@95% CL Below Mass Scale of Λ/g**



SM is red square. Dashed contours indicate value of $\Lambda/g = 3, 5,$ and 8 TeV.
(^{133}Cs APV, from PDG – Flambaum)

θ_h is “flavor mixing angle” in Lagrangian $\mathcal{L}_{\text{NP}}^{\text{PV}}$ for new physics at value Λ/g mapped around boundary of experimental limits.

SM Tests: Past & Future Precision Low Energy Parity Violation Measurements

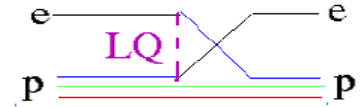
Λ/g lower limits@95% CL using formalism of
 Erler, *et al.*, *Ann. Rev. Nucl. Part. Sci* **64**, 269, (2014)

Experiment	% Precision	$\Delta\sin^2 \theta_w$	Λ/g [TeV] (mass reach)
SLAC-E122	8.3	0.011	1.5
SLAC-E122	110	0.44	0.25
APV (^{205}Tl)	3.2	0.011	3.8
APV (^{133}Cs)	0.58	0.0019	9.1
SLAC-E158	14	0.0013	4.8
Jlab-Hall A	4.1	0.0051	2.2
Jlab-Hall A	61	0.051	0.82
JLab-Qweak (p)	6.2	0.0011	7.5
JLab-SoLID	0.6	0.00057	6.2
JLab-MOLLER	2.3	0.00026	11.0
Mainz-P2	2.0	0.00036	13.8
APV ($^{225}\text{Ra}^+$)	0.5	0.0018	9.6
APV ($^{213}\text{Ra}^+ / ^{225}\text{Ra}^+$)	0.1	0.0037	4.5
PVES (^{12}C)	0.3	0.0007	14

published

planned

Leptoquarks



- Impact on $Q_W(p)$ of leptoquarks was explored by Erler, Kurylov, Ramsey-Musolf, Phys. Rev. D **68**, 016006 (2003)
- Analysis a bit dated (2003), but suggestive; included HERA, LEP, and APV data (missing more recent HERA data; see Aaron, et al. Phys. Lett. B **705**, 52 (2011).)

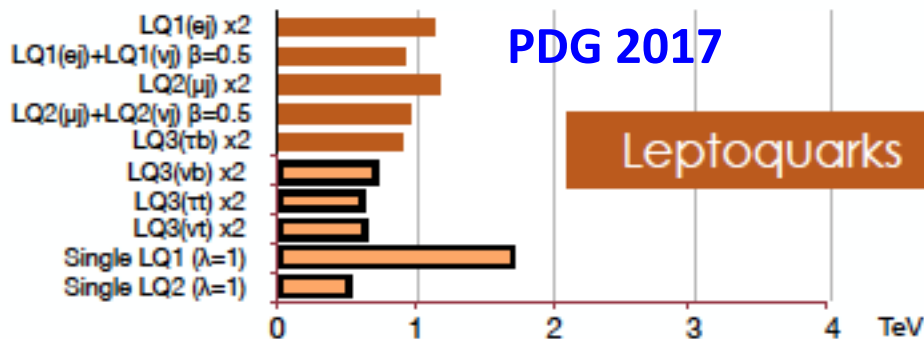
Leptoquarks

New Q_{weak} data (6.2% 1σ error) has sensitivity to distinguish among LQ types at 95% CL

Scalar Leptoquarks

Vector Leptoquarks

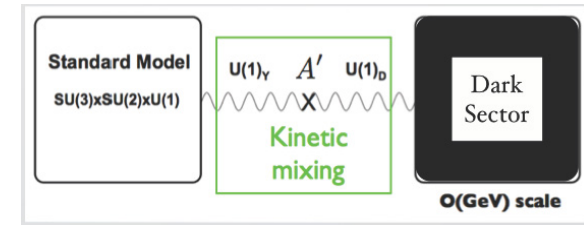
LQ	Consistency	$\Delta Q_W(p)/Q_W(p)$	LQ	Consistency	$\Delta Q_W(p)/Q_W(p)$
S_1^L	0.57	9%	$U_{1\mu}^L$	0.26	-8%
S_1^R	0.01	-6%	$U_{1\mu}^R$	0.56	6%
\tilde{S}_1^R	0.44	-6%	$\tilde{U}_{1\mu}^R$	0.99	25%
S_3	0.76	10%	$U_{3\mu}$	0.31	-4%
R_2^L	0.44	-13%	$V_{2\mu}^L$	0.87	9%
R_2^R	0.89	15%	$V_{2\mu}^R$	0.11	-7%
\tilde{R}_2^L	0.13	-4%	$\tilde{V}_{2\mu}^L$	0.56	14%



- LHC limits currently at ~ 1 TeV
- Low energy precision data continues to play important role in recent analyses including LHC data: see Phys. Rep. **641**, 1 (2016)

Dark Photon – Sensitivity to MeV scale Mediators

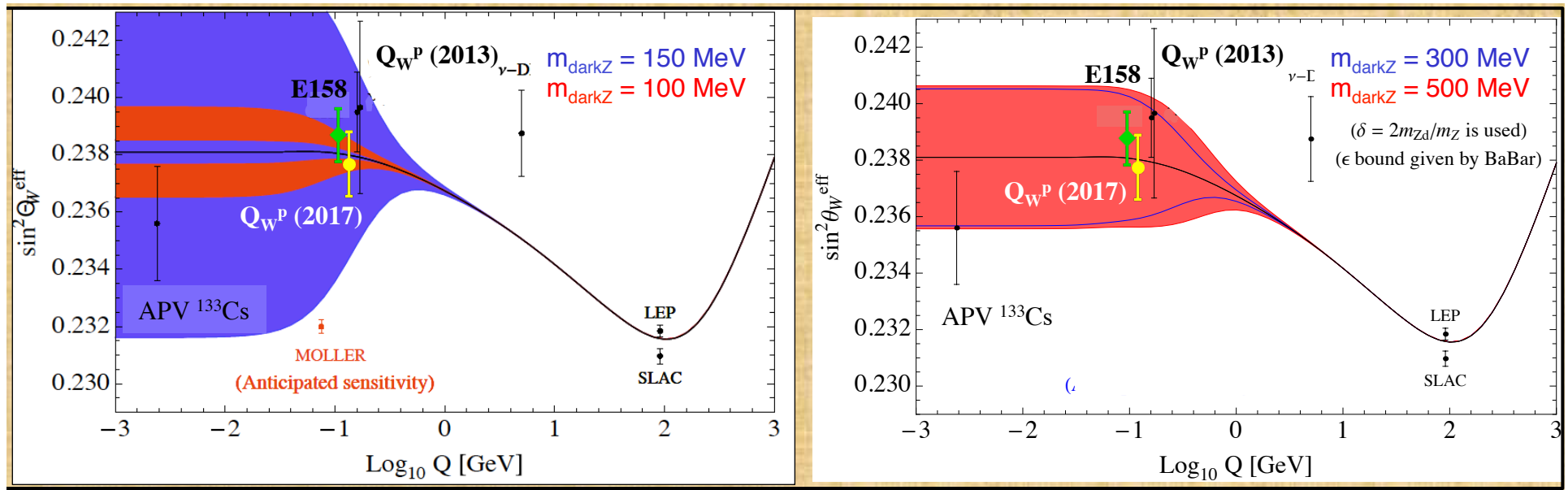
“Dark photon” – possible portal for new force to communicate with SM



“Dark parity violation”

(Davoudiasl, Lee, Marciano, Phys. Rev. D **89**, 095006 (2014))

- New source of low energy parity violation through mass mixing between Z_0 and Z_d
- Complementary to direct searches for heavy dark photons; observable even if direct decay modes are “invisible”
- Example: possible deviations of $\sin^2\theta_W$ for dark photons respecting rare kaon decay constraints and muon $g-2$ is explained
- **New Q_{weak} point rules out some of the allowed region**

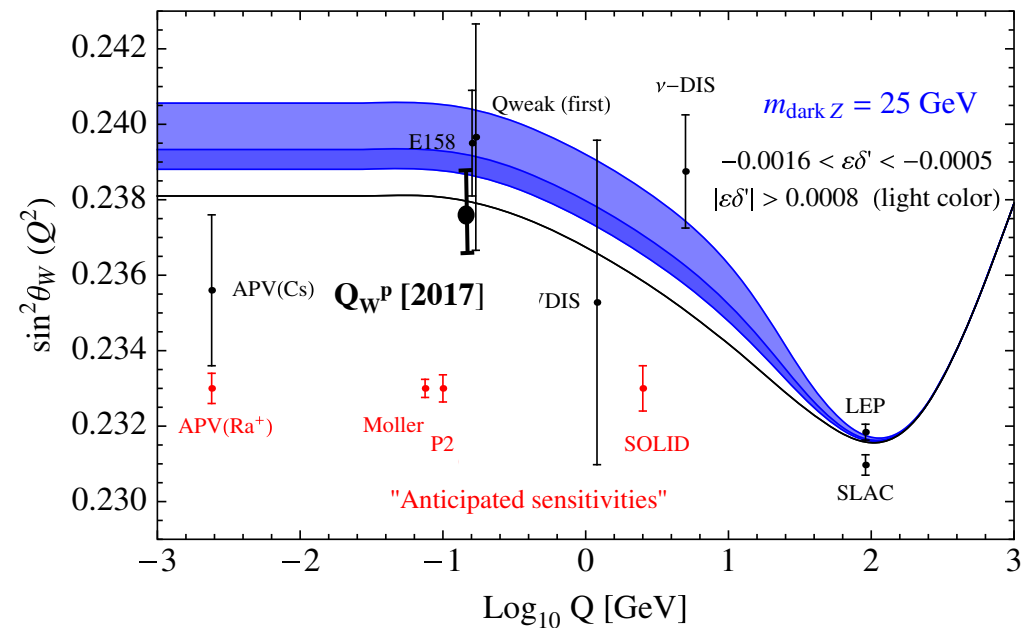
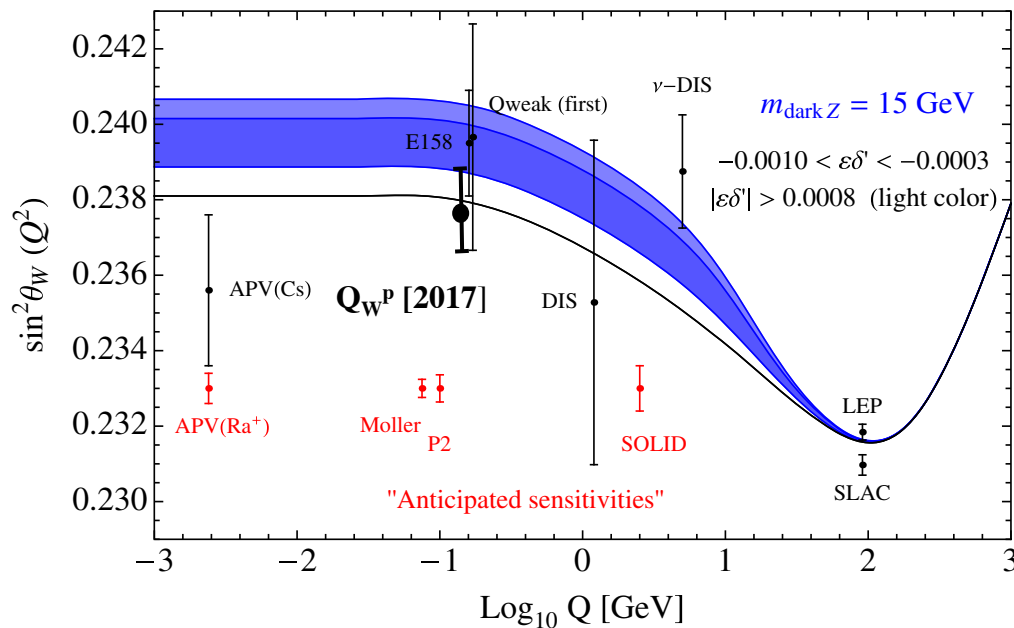


Dark Photon – Sensitivity to GeV scale Mediators

- Davoudiasl, Lee, Marciano, Phys. Rev. D **92**, 055005 (2015) discussed intermediate mass (10 – 35 GeV) dark Z bosons Z_d
- In contrast to the lighter variety, these would show signatures both in low energy PV (shift of weak mixing angle) and in rare Higgs decays or direct Drell-Yan production at LHC

$$H \rightarrow Z Z_d \text{ or } H \rightarrow Z_d Z_d \quad pp \rightarrow Z_d X$$

- The specific bands were influenced by the NuTeV result, but the new Q_{weak} data disfavors that region



Ancillary Measurements

Qweak made several ancillary measurements to determine and constrain background processes and corrections – many will result in physics publications

- PV asymmetry:
 - elastic ^{27}Al
 - $\text{N} \rightarrow \Delta$
($E = 1.16 \text{ GeV}, 0.877 \text{ GeV}$)
 - Near $W = 2.5 \text{ GeV}$
(related to γZ box)
 - Pion photoproduction
($E = 3.3 \text{ GeV}$)
- PC Transverse asymmetry:
 - elastic ep
 - elastic ^{27}Al , Carbon
 - $\text{N} \rightarrow \Delta$
 - Møller
 - Near $W = 2.5 \text{ GeV}$
 - Pion photoproduction
($E = 3.3 \text{ GeV}$)

Conclusion

Q_{weak} **experiment** – precision measurement of parity-violating asymmetry in elastic e-p scattering → proton's weak charge

$$A_{ep} = -226.5 \pm 7.3(\text{stat}) \pm 5.8(\text{syst}) \text{ ppb at } \langle Q^2 \rangle = 0.0249 \text{ (GeV / c)}^2$$
$$Q_W^p(\text{this expt.}) = 0.0719 \pm 0.0045 \quad Q_W^p(\text{SM}) = 0.0708 \pm 0.0003$$

Implications:

- Measured proton weak charge in good agreement with Standard Model
- Completes the “weak charge triad” of high precision low energy weak charge measurements
- Bounds on new neutral current semi-leptonic PV physics:
 - amplitudes above $\sim 8 \times 10^{-3} G_F$ ruled out at 95% CL
 - mass/coupling scales of heavy new physics ruled out at $\Lambda/g < 7.5 \text{ TeV}$ at 95% CL (following Erler, *et al.* arXiv:1401.6199 prescription)
 - for $g^2 = 4\pi$ (maximal contact interaction coupling) $\Lambda = 26.5 \text{ TeV}$
 - Will play a role in future analyses of bounds (or discoveries) of a variety of new physics
- Provides scientific and technical developments for next generation of measurements to build on

The Qweak Collaboration

101 collaborators 26 grad students
11 post docs 27 institutions

Institutions:

- 1 University of Zagreb
- 2 College of William and Mary
- 3 A. I. Alikhanyan National Science Laboratory
- 4 Massachusetts Institute of Technology
- 5 Thomas Jefferson National Accelerator Facility
- 6 Ohio University
- 7 Christopher Newport University
- 8 University of Manitoba,
- 9 University of Virginia
- 10 TRIUMF
- 11 Hampton University
- 12 Mississippi State University
- 13 Virginia Polytechnic Institute & State Univ
- 14 Southern University at New Orleans
- 15 Idaho State University
- 16 Louisiana Tech University
- 17 University of Connecticut
- 18 University of Northern British Columbia
- 19 University of Winnipeg
- 20 George Washington University
- 21 University of New Hampshire
- 22 Hendrix College, Conway
- 23 University of Adelaide
- 24 Syracuse University
- 25 Duquesne University



D. Androic,¹ D.S. Armstrong,² A. Asaturyan,³ T. Averett,² J. Balewski,⁴ **K. Bartlett,**² J. Beaufait,⁵ **R.S. Beminiwattha,**⁶ J. Benesch,⁵ F. Benmokhtar,^{7,25} J. Birchall,⁸ **R.D. Carlini,**^{5,2} G.D. Cates,⁹ **J.C. Cornejo,**² S. Covrig,⁵ M.M. Dalton,⁹ C.A. Davis,¹⁰ W. Deconinck,² J. Diefenbach,¹¹ **J.F. Dowd,**² J.A. Dunne,¹² D. Dutta,¹² **W.S. Duvall,**¹³ M. Elaasar,¹⁴ W.R. Falk*,⁸ J.M. Finn*,² T. Forest,^{15,16} C. Gal,⁹ D. Gaskell,⁵ M.T.W. Gericke,⁸ J. Grames,⁵ **V.M. Gray,**² K. Grimm,^{16,2} **F. Guo,**⁴ **J.R. Hoskins,**² K. Johnston,¹⁶ **D. Jones,**⁹ M. Jones,⁵ R. Jones,¹⁷ **M. Kargiantoulakis,**⁹ P.M. King,⁶ E. Korkmaz,¹⁸ **S. Kowalski,**⁴ **J. Leacock,**¹³ **J. Leckey,**² **A.R. Lee,**¹³ J.H. Lee,^{6,2} L. Lee,¹⁰ **S. MacEwan,**⁸ D. Mack,⁵ **J.A. Magee,**² R. Mahurin,⁸ J. Mammei,¹³ J.W. Martin,¹⁹ **M.J. McHugh,**²⁰ D. Meekins,⁵ J. Mei,⁵ R. Michaels,⁵ A. Micherdzinska,²⁰ A. Mkrтчhyan,³ H. Mkrтчhyan,³ N. Morgan,¹³ **K.E. Myers,**²⁰ **A. Narayan,**¹² L.Z. Ndukum,¹² V. Nelyubin,⁹ **H. Nuhait,**¹⁶ **Nuruzzaman,**^{11,12} W.T.H van Oers,^{10,8} A.K. Opper,²⁰ **S.A. Page,**⁸ **J. Pan,**⁸ K.D. Paschke,⁹ S.K. Phillips,²¹ M.L. Pitt,¹³ M. Poelker,⁵ J.F. Rajotte,⁴ W.D. Ramsay,^{10,8} J. Roche,⁶ B. Sawatzky,⁵ T. Seva,¹ M.H. Shabestari,¹² R. Silwal,⁹ N. Simicevic,¹⁶ **G.R. Smith,**⁵ P. Solvignon*,⁵ D.T. Spayde,²² **A. Subedi,**¹² R. Subedi,²⁰ R. Suleiman,⁵ V. Tadevosyan,³ W.A. Tobias,⁹ V. Tvaskis,^{19,8} **B. Waidyawansa,**⁶ **P. Wang,**⁸ S.P. Wells,¹⁶ S.A. Wood,⁵ **S. Yang,**² R.D. Young,²³ **P. Zang,**²⁴ and S. Zhamkochyan³

Upcoming Q_{weak} Conference Talks

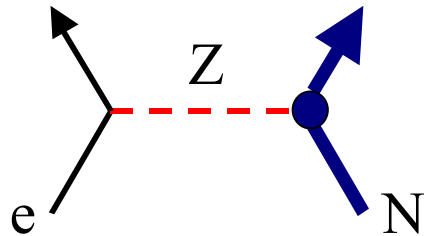
- PANIC 2017, Sept. 1 – 5, 2017, Beijing, China, **Roger Carlini**
- TRIUMF, Sept. 7, 2017, **Michael Gericke**
- JLab, Sept. 8, 2017, **Mark Pitt**
- HADRON 2017, Sept. 25 – 29, 2017, Salamanca, Spain, **Paul King**
- LASNPA 2017, Oct. 23 - 27, 2017, Havana, Cuba, **Neven Simicevic**
- DNP Fall Meeting, Oct. 25 – 28, 2017, Pittsburgh, PA, **Greg Smith**
- EINN 2017, Oct. 29 – Nov. 4, 2017, Paphos, Cyprus, **David Armstrong**
- SESAPS, Nov. 16 – 18, 2017, Midgeville, GA, **Valerie Gray**

End

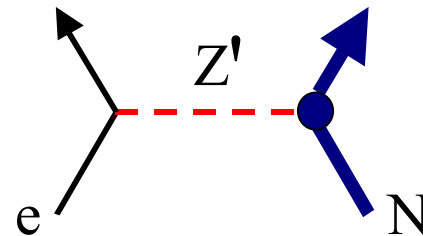
Backups

Why are Precision Measurements far Below the Z-pole Sensitive to New Physics?

Precision measurements well below the Z-pole have more sensitivity (for a given experimental precision) to new types of tree level physics, such as additional heavier Z' bosons.



$$A_Z \propto \frac{g^2}{-q^2 + M_Z^2 + iM_Z\Gamma_Z}$$



$$A_{Z'} \propto \frac{g^2}{-q^2 + M_{Z'}^2 + iM_{Z'}\Gamma_{Z'}} \xrightarrow{q^2 \ll M_{Z'}^2} \frac{g^2}{M_{Z'}^2}$$

At Z-pole, $q^2 \sim M_Z^2$, $A \sim \frac{1}{M_Z\Gamma_Z} + \frac{1}{M_{Z'}^2}$, $\sim 0.1\%$ precision $\rightarrow M_{Z'} < 500$ GeV

At low energy, $q^2 \ll M_Z^2$, $A \sim \frac{1}{M_Z^2} + \frac{1}{M_{Z'}^2}$, $\sim 0.1\%$ precision $\rightarrow M_{Z'} < 2.5$ TeV

